Cellular and Molecular Life Sciences (2025) 82:218
https://doi.org/10.1007/s00018-025-05746-1

ORIGINAL ARTICLE

Dual phosphorylation of glycogen synthase kinase 3β differentially integrates metabolic programs to determine T cell immunity across vertebrates

Wei Liang[1] · Ming Geng[1] · Wenzhuo Rao[1] · Kang Li[1] · Yating Zhu[1] · Yuying Zheng[1] · Xiumei Wei[1] · Jialong Yang[1,2]

Received: 28 March 2025 / Revised: 8 May 2025 / Accepted: 9 May 2025

Abstract

The integration of metabolic programs with T cell signaling establishes a molecular foundation for immune metabolism. As a key metabolic regulator, GSK3β's activity is dynamically modulated by phosphorylation at Ser9 and Tyr216. However, the contribution of these phosphorylation sites on metabolism-driven T cell response remains unclear. Using tilapia and mouse models, we investigated the regulation of GSK3β on T cell metabolism and its evolutionary variation. In tilapia, T cell activation induces GSK3β signaling, linking to both glycolysis and oxidative phosphorylation (OXPHOS). Tyr216 phosphorylation preferentially promotes glycolysis, facilitating T cell activation, proliferation, and antibacterial immunity; while inhibition of Ser9 phosphorylation specifically enhances OXPHOS to sustain T cell responses. Differently, Tyr216 phosphorylation supports both glycolysis and OXPHOS in mouse, ensuring $CD4^+$ T and $CD8^+$ T cell activation, proliferation, and cytokine production. Although Ser9 phosphorylation controls OXPHOS, its inhibition impairs rather than enhances OXPHOS and $CD4^+$ T cell responses in mouse. We thus revealed a previously unknown mechanism underlying T cell metabolism and proposed that, through evolution, GSK3β has restructured the regulatory strategy, enabling bidirectional control of T cell metabolism and immunity in mammals and enhancing the flexibility of the adaptive immune system.

Keywords GSK3β · T cells · Evolution · Immunometabolism · Fish

Introduction

T cells are essential components of the adaptive immune system, playing a critical role in resisting pathogen invasion, maintaining immune homeostasis, and tumor surveillance [1]. There is a growing recognition that T cell immunity is intimately linked to metabolism. Metabolic programs supply energy for T cells and ensure their proliferation and effector functions through the biosynthesis of nucleotides, fatty acids, proteins, and other molecules [2]. T cells at different stages exhibit distinct metabolic properties and dynamically rewire their metabolic programs to meet functional demands [3, 4]. Naive T cells predominantly rely on fatty acid oxidation (FAO) and oxidative phosphorylation (OXPHOS) for energy. Upon activation, T cells rapidly shift their metabolism to favor fatty acid synthesis (FAS), glycolysis, and glutaminolysis, with an enhanced level of OXPHOS. Dysfunction in these metabolic programs or the reprogramming severely impairs T cell immunity [5]. For instance, glycolysis and glutaminolysis integrate with mTORC1 signaling to regulate T cell immunity [6]; blocking these metabolic programs cripples $CD4^+$ T cell proliferation and their ability to differentiate into Th1 and Th17 lineages [7–9], while also compromising $CD8^+$ T cell cytotoxicity [10]. Whereas,

Wei Liang, Ming Geng and Wenzhuo Rao contributed equally to this work.

✉ Xiumei Wei
xmwei@bio.ecnu.edu.cn

✉ Jialong Yang
jlyang@bio.ecnu.edu.cn

[1] State Key Laboratory of Estuarine and Coastal Research, School of Life Sciences, East China Normal University, Shanghai 200241, China

[2] Laboratory for Marine Biology and Biotechnology, Qingdao Marine Science and Technology Center, Qingdao 266237, China

Published online: 28 May 2025

inhibition of FAO disrupts the Th17/Treg balance, driving $CD4^+$ T cells to favor the Th17 lineage over the Treg direction [9]. These findings underscore the paramount importance of metabolism in determining T cell immune fate and function.

The integration of metabolic transporters, enzymes, and transcription factors with T cell signaling establishes the molecular foundations underlying the regulation of metabolism in T cell immunity. Glycogen synthase kinase 3 beta (GSK3β) is an evolutionarily conserved serine/threonine kinase whose activity is dynamically regulated by two phosphorylation sites, Ser9 and Tyr216 [11]. Phosphorylation at Tyr216 enhances GSK3β's ability to bind and phosphorylate substrates, while phosphorylation at Ser9 inhibits GSK3β activity [12]. Recent evidence has highlighted the critical role of GSK3β in regulating cellular metabolism. Inhibition of Ser9 phosphorylation enhances mTOR activity, upregulates Glut1 expression, and increases glucose uptake in vascular smooth muscle cells, thereby facilitating protein and fatty acid synthesis for cell growth [13]. Conversely, increased phosphorylation at Ser9 leads to an accumulation of reactive oxygen species (ROS), impairs chondrocyte proliferation, and accelerates cellular aging [14]. Unlike Ser9, blocking Tyr216 phosphorylation weakens AMPK/mTOR-mediated glycolysis but enhances mitochondrial respiration, OXPHOS, and FAO [15]. These observations suggest that GSK3β may regulate various metabolic programs via the phosphorylation of two distinct sites. However, whether these two phosphorylation sites have preferences or specificities in regulating metabolic programs remains unknown.

As a central hub for many signaling molecules, GSK3β intimately coordinates several pathways and transcription factors to orchestrate T cell function and fate. Blocking Tyr216 phosphorylation impairs T-bet nuclear translocation, resulting in defective T cell activation, Th1 cell differentiation, and cytokine production [16]. In contrast, inhibition of Ser9 phosphorylation boosts the proliferation and IL-2 production of $CD4^+$ memory T cells while enhancing T-bet-controlled $CD8^+$ T cell cytotoxicity [17, 18]. However, whether GSK3β regulates T cell immunity by coupling metabolic programs remains unclear. We also lack understanding of whether its phosphorylation sites differentially determine the immune outcome of T cells by specifically linking distinct metabolic programs. Furthermore, it remains unknown whether the integration between GSK3β-controlled metabolism and T cell immunity is independently acquired by mammals or represents a gradually evolved strategy common to vertebrates. Answering these questions will provide novel insights into the crosstalk between immunity and metabolism, as well as the evolution of this strategy.

Fish are the lowest extant vertebrates possessing T cells. To date, $CD4^+$ and $CD8^+$ T cells, as well as T cell subsets such as Th1, Th17, and Treg, have been identified in at least ten teleost species, including zebrafish, tilapia, grass carp, and Japanese flounder [19–22]. The crucial roles of T cells in fish for combating pathogen infections and repairing tissue damage have also been elucidated. Similar to mammals, the immune response of fish T cells is intricately regulated. For instance, the large yellow croaker utilizes IL-2 coupled with the STAT5, MAPK/Erk, and mTORC1 pathways to promote T cell proliferation [23]. Tilapia facilitates antibacterial immunity in T cells via calcium influx-controlled NFAT nuclear translocation, NF-κB coupled IL-17 A signaling, and the IL-2/mTORC1 axis-manipulated Th1 cell differentiation [20, 24, 25]. Importantly, we found that mTORC1, MAPK/Erk, and c-Myc collectively ensure the activation, proliferation, and effector functions of tilapia T cells by maintaining metabolic reprogramming, glycolysis and glutaminolysis, respectively [26–28]. This highlights the indispensable role of metabolic programming in fish T cell immunity. As a central hub regulating cellular metabolism and proliferation, GSK3β modulates protein synthesis in the muscle cells of zebrafish via the TSC2/mTOR pathway [29]. Inhibition of Ser9 phosphorylation significantly reduces lipid accumulation in the liver of schizothorax, large yellow croaker, and zebrafish [30–32]. However, as in mammals, the correlation between GSK3β-controlled metabolic programs and T cell immunity remains completely unknown in fish. Therefore, combining mammalian and fish models provides an ideal approach to elucidate the GSK3β-driven T cell immunometabolism, not only as a previously unknown defense strategy, but also for its evolutionary pattern.

In this study, we found that activated T cells in tilapia initiate the PI3K-AKT pathway to activate GSK3β, which then triggers both glycolysis and OXPHOS. Tyr216 phosphorylation prefers glycolysis, whereas inhibiting Ser9 phosphorylation favors OXPHOS. The crosslinking of these two sites to distinct metabolic pathways dynamically controls T cell activation and anti-infective immunity, representing a previously unknown mechanism of T cell immunometabolism. Interestingly, we found that Tyr216 phosphorylation in mouse GSK3β gains the ability to modulate OXPHOS while maintaining its regulatory capacity for glycolysis, thus ensuring T cell activation, proliferation, and cytokine production. Although Ser9 in mouse GSK3β similarly links to OXPHOS, inhibition of its phosphorylation impairs OXPHOS and T cell immunity, contrasting with the findings in tilapia. We therefore propose that during evolution, mammalian GSK3β had reshaped the strategy of regulating T cell immunity via metabolic programs, acquiring the dual-efficacy pathways to determine immune defense. This adaptation benefits mammals by creating a more flexible and sophisticated immune regulation.

Materials and methods

Ethics statement

All experimental procedures were conducted in accordance with the Guide for the Care and Use of Laboratory Animals of the Ministry of Science and Technology of China. This study was approved by the East China Normal University Experimental Animal Ethics Committee with a number of AR2024-085.

Experimental animals

Nile tilapia larvae were purchased from an aquatic farm in Guangzhou, Guangdong Province, China, and were cultured in a circulating water system at 28 °C with continuous aeration, at the Biological Station of East China Normal University. Tilapia individuals about 10 cm were used for the corresponding experiments. BALB/c mice were purchased from and kept in Minhang Laboratory Animal Center of East China Normal University.

Sequence, structure, and phylogenic analysis

The cDNA or amino acid sequences of related genes were obtained from NCBI GenBank, and were subject to the BLAST algorithm analysis. The functional domains were predicted using the Simple Modular Architecture Research Tool (SMART, http://smart.embl-heidelberg.de/) and were displayed with DOG version 2.0 software. The multiple sequences alignment of amino acid was performed by the ClustalW. The protein tertiary structures were predicted by the SWISS-MODEL (https://www.swissmodel.expasy.org/), and displayed with PyMOL software. The phylogenetic tree was constructed using MEGA 7.0 software with the neighbor-joining algorithm, and bootstrap values of 1000 replicates (%) were indicated for the branches. The accession numbers of all selected genes were listed in Table S1.

Bacterial infection

Edwardsiella piscicida was cultured in TYB medium at 28 °C, and was collected, washed and resuspended in sterile PBS to a concentration of 1×10^6 CFU/mL. Each tilapia was intraperitoneally (*i.p.*) injected with 200 μL *E. piscicida* suspension, and the control group was injected with the same volume of sterile PBS. To determine the bacterial titers, the livers of infected tilapia were harvested and grinded, and the bacterial colonies on TYB agar plates were calculated.

Leukocytes isolation

Spleen leukocytes of tilapia were isolated according to our previous report [26]. Briefly, spleens were harvested and grinded in Leibovitz's L-15 medium (Gibco). Percoll solution was prepared by mixing Percoll (GE Healthcare) with 10 × PBS at a 9:1 ratio, and diluted to 34% and 52% Percoll with L-15 medium, respectively. The cell suspension was filtered with nylon mesh and added onto a 52%/34% discontinuous density-gradient Percoll, and centrifuged at 500 g for 35 min with the lowest acceleration and deceleration. Leukocytes between 52% and 34% Percoll were collected, washed and resuspended in L-15 medium (10% FBS) for indicated assays. These isolated spleen leukocytes were considered as spleen lymphocytes, because more than 90% of these cells belong to the lymphocyte population [26, 28, 33]. To isolate splenocytes of mouse, spleens were ground and treated with ACK buffer to remove red blood cells, and then washed and resuspended in DMEM (10% FBS, 1% penicillin and streptomycin) for further assays.

Leukocytes stimulation

For T cell activation, the spleen leukocytes of tilapia were stimulated with 2 μg/mL mouse anti-tilapia CD3ε mAb plus mouse anti-tilapia CD28 mAb [34], and cultured in DMEM (10% FBS and 1% penicillin/streptomycin) at 28 °C for indicated time points. To address T cell activation signaling, the spleen leukocytes were resuspended in Dulbecco's PBS at incubated at 28 °C for 30 min to rest the phosphorylated protein. After that, the cells were stimulated with 2 μg/mL mouse anti-tilapia CD3ε/CD28 mAb or 50 ng/mL phorbol 12-myrustate 13-acetatae (PMA, MedChemExpress) plus 500 ng/mL ionomycin (MedChemExpress) (P + I), and cultured as above for indicated time. For mouse splenocytes stimulation, the cells were activated by 2 μg/mL of anti-mouse CD3ε (BioLegend) plus anti-mouse CD28 (BioLegend) or P + I as above.

RNA-Seq assay

The spleen leukocytes of tilapia were stimulated with CD3ε/CD28 mAbs as above for 0, 12 or 24 h, and four biological replicates were performed for each group. Then, the cells were harvested to extract total RNA with Trizol reagent (Invitrogen). The RNA concentrations were examined by NanoDrop 2000, and the samples were sent to Genedenovo company (Guangzhou, China) for RNA-Seq assay. RNA-Seq, data generation and normalization were performed on the Illumina Cluster Station and Illumina HiSeq 2000 System. The analysis of differentially expressed genes, GO and

KEGG pathway enrichment were performed as our previous studies [28].

Quantitative real-time RT-PCR (qPCR)

Total RNA was extracted with Trizol reagent (Invitrogen), treated with gDNA Purge (Novoprotein), and then was reverse-transcribed by the first-strand cDNA synthesis supermix (Novoprotein). The 1:30 diluted cDNA production was used as template for qPCR assay with NovoStart SYBR qPCR SuperMix Plus (Novoprotein) on CFX Connect Real-Time System (Bio-Rad). β-actin was used as reference gene, and the relative mRNA expression of target genes were analyzed with $2^{-\Delta\Delta CT}$ method. The gene-specific primers used were listed in Table S2.

Dual luciferase assay

Promoter region of tilapia GSK3β was cloned into the pGL3 vector, and the full-length coding region of AKT1 was cloned into the pcDNA3.1 vector. 200 ng AKT1-pcDNA3.1 and GSK3β-pGL3 promoter plasmids were co-transfected into 2 × 10 HEK 293 T cells according using Lipofectamine 2000 (Invitrogen). At 4 h after transfection, the medium was replaced with DMEM. Cells were collected and lysed using passive lysis buffer (Promega) at 48 h post transfection, and the luciferase activity was measured according to the Dual-Luciferase Reporter Assay System (Promega).

Inhibitor treatment

For in vitro inhibition, 10 μM oridonin (AKT inhibitor, MedchemExpress), 30 μM Chir99021 (GSK3β Tyr216 inhibitor, MedchemExpress), 30 μM SB216763 (GSK3β Ser9 inhibitor, MedchemExpress), 3 μM 2-DG (Heoxkinase inhibitor, MedchemExpress) or 30 μM Antimycin A (Cytochrome C inhibitor, Chemical BooK) were added into the spleen leukocytes of tilapia and cultured with DMEM (10% FBS) for 3 h. Then, the cells were stimulated with CD3ε/CD28 mAbs as above for assay. To inhibit GSK3β phosphorylation in vivo, tilapia individuals were *i.p.* injected with 2 mg/kg Chir99021 or 3.71 mg/kg SB216763 for 2 consecutive days before bacterial infection.

Pyruvate rescue assay

Tilapia spleen leukocytes were treated with 30 μM of Chir99021 for 3 h to inhibit GSK3β Tyr216 phosphorylation, before the cells were stimulated with CD3ε/CD28 mAb as described with or without 5 μM of pyruvate (Sangon Biotech). The cells were then cultured in DMEM (10% FBS) at 28 °C for indicated time for assays.

Western blot

Tilapia spleen leukocytes or mouse splenocytes were lysed in NP40 lysis buffer containing 1 mM PMSF, 1% Protease Inhibitor Cocktail and 1% Phosphatase Inhibitor Cocktail III on the ice for 30 min. After being centrifugated at 1000 rpm for 10 min, the supernatant was collected for assay. The nuclear protein was extracted using a commercial kit (Beyotime Biotechnology). The samples were mixed with SDS-loading buffer, boiled at 100 °C for 8 min, separated by SDS-PAGE and transferred onto nitrocellulose membrane. After blocking with 4% non-fat powder milk in PBST (PBS containing 0.05% Tween-20) at room temperature for 1 h, the membrane was probed with 1:1000 diluted antibodies for p-Erk1/2 (Thr202/Tyr204), total Erk1/2, PI3Kinase p110α, p-AKT (Ser473), total AKT, p-GSK3β (Ser9), p-AMPKα (Thr172), total AMPKα, p-mTOR (Ser2448), total mTOR, p-S6 (Ser240/244), total S6, p-4E-BP1 (Thr37/46), total 4E-BP1, c-Myc, cleaved Caspase-3 and β-actin purchased from Cell Signaling Technology, or antibodies for p-GSK3β (Tyr216), total GSK3β, Hexokinase II, PFK, PKM, Glut1, PGC-1α, Cytochrome C (Cyc1), Nrf1, and TFAM purchased from Beyotime Biotechnology at 4 °C overnight. The membrane was washed three times with PBST, and incubated with 1:30,000 diluted Alexa Fluor 800-conjugated goat anti-rabbit IgG H&L (Cell Signaling Technology) or 1:10000 diluted Alexa Fluor 680-conjugated goat anti-mouse IgG H&L (Abcam) at room temperature for 1 h. After washing with PBST, the membrane was scanned by Odyssey CLx Image Studio.

GSK3β overexpression

The coding region of tilapia GSK3β was amplified from tilapia cDNA and cloned into pEGFP-C1 plasmid to construct transfection vectors. HEK 293 T cells were transfected with GSK3β-pEGFP-C1 plasmid, with pEGFP-C1 plasmid as control group. At 48 h post-transfection, the cells were lysed in NP40 lysis buffer on ice for 30 min, and supernatants were subjected to Western blot assay.

Co-immunoprecipitation (Co-IP) assay

The coding region of tilapia AKT and GSK3β with Flag or HA tags were amplified from tilapia cDNA, and clone into pEGFP-C1 plasmid to construct transfection vectors. Then, 5 μg AKT-HA-pEGFP-C1 and GSK3β-Flag-pEGFP-C1 plasmids were co-transfected into 2×10^6 HEK 293 T cells. At 48 h after transfection, cells were lysed in NP40 lysis buffer on ice for 30 min. The supernatants were collected and incubated with 10 μL Flag Ab-conjugated agarose beads (Sigma-Aldrich) at 4 °C overnight with shaking. After

washing four times with NP40 lysis buffer, the beads were mixed with SDS-loading buffer and heated at 100 ˚C for 10 min. The supernatants were used for Western blot assay.

Flow cytometry

Tilapia spleen leukocytes were resuspended in FACS buffer (PBS with 2% FBS) and stained with FITC-conjugated mouse anti-tilapia CD3ε on the ice for 30 min [28], and then washed twice with FACS buffer. For intracellular staining of tilapia T cells, after staining with CD3ε as above, the cells were fixed with BD Cytofix/Cytoperm buffer on ice for 30 min and washed twice using BD Perm/Wash Buffer, and then stained with 1:400 diluted APC-conjugated anti-p-ERK1/2 Thr202/Thy204 (BioLegend) on ice for 30 min. Mouse splenocytes were stained with 1:400 diluted PE/Cyanine7-conjugated anti-mouse CD4 (BioLegend), PE-conjugated anti-mouse CD8α (BioLegend) and APC-conjugated anti-mouse CD69 (BioLegend) on ice for 20 min. For cytokine staining in mouse T cells, the P + I stimulated splenocytes were stained with CD4 and CD8α as above, and then fixed with BD Cytofix/Cytoperm Buffer as previously described. The cells were then stained with a 1:400 diluted APC-conjugated anti-mouse IL-2 (BioLegend), Brilliant Violet 421-conjugated anti-mouse IFN-γ (BioLegend) or FITC-conjugated anti-mouse TNF-α (BioLegend) in Perm/Wash buffer on ice for 30 min. All samples were washed two times with FACS buffer or Perm/Wash Buffer, collected on BD CantoII flow cytometer and analyzed by FlowJo software.

Glucose uptake assay

The spleen leukocytes of tilapia were stained by mouse anti-tilapia CD3ε as above. Subsequently, the cells were resuspended with PBS in 96-well plates, and incubated with 100 μM fluorescent 2-(N-(7-nitrobenz-2-oxa-1,3-diazol-4-yl) amino)−2-deoxyglucose (2-NBDG; Life Technologies) at 28 ℃ for 30 min. The cells were washed two times with prechilled PBS, and followed by flow cytometry assay.

5-Bromodeoxyuridinc (BrdU) incorporation

Tilapia individuals were infected with *E. piscicida* and treated with or without Chir99021 as above. On day 3 after infection, the animals were *i.p.* injected with 0.075 g/Kg of BrdU in 200 μL of PBS. Spleen leukocytes were isolated 24 h later. After stained with mouse anti-tilapia CD3ε as described above, the cells were fixed with BD Cytofix/Cytoperm Buffer on ice for 30 min, followed by washed two times with BD Perm/Wash Buffer. The cells were then permeabilized with BD Cytoperm Plus Buffer on ice for 10 min, washed two times, and re-fixed with BD Cytofix/Cytoperm Buffer on ice for another 5 min. After treated with 300 μg/mL DNase at 37 ℃ for 1 h, the samples were stained with 1:100-diluted APC-conjugated anti-BrdU antibody (BD, Biosciences) in Perm/Wash buffer at room temperature for 20 min. The samples were washed two times and analyzed by flow cytometry.

In vitro proliferation assay

1×10^6 cells of tilapia spleen leukocytes or mouse splenocytes were stained with 10 μM CFSE (Invitrogen) at room temperature for 10 min. After washing twice with L-15 medium, cells were resuspended with DMEM (10% FBS) and cultured in 24-well plates with the addition of 2 μg/mL anti-tilapia or anti-mouse CD3ε/CD28 mAbs. Cells were harvested at 48 h to stain CD3ε, CD4 or CD8 as described above. Subsequently, 1:400-diluted 7-AAD (Invitrogen) was added before analyzing by the flow cytometry.

Apoptosis assay

The spleen leukocytes of tilapia were stained with mouse anti-tilapia CD3ε mAb as above. Then, the cells were stained with 1:400-diluted Annexin V antibody (BioLegend) in Annexin V binding buffer (0.14 M NaCl, 0.01 M HEPES/NaOH, 2.5 mM $CaCl_2$, pH 7.4,) at room temperature for 15 min. Finally, 1:400-diluted 7-AAD were added before the samples were analyzed by flow cytometry.

Examination of enzyme activity

Spleen leukocytes of tilapia were stimulated with CD3ε/CD28 mAbs in the presence or absence of indicated inhibitors for different time points. The activities of Hexokinase (HK), pyruvate kinase (PKM) and reactive oxygen (ROS) were examined by the commercial assay kits purchased from Nanjing Jiancheng Bioengineering Institute. The activities of Mitochondrial membrane (JC-1) were detected by the commercial assay kits purchased from Solarbio company.

Statistical analysis

The results were presented as mean ± standard error of mean (SEM), and significant difference were determined by a two-tailed Student t-test. p values were defined as follows: *, $p < 0.05$; **, $p < 0.01$; ***, $p < 0.001$.

Results

T cell activation in tilapia is associated with glycolysis and mitochondrial OXPHOS

Spleen leukocytes of tilapia were stimulated with CD3ε/CD28 mAbs and subjected for RNA-Seq. The inducible expression of CD122 (IL-2Rβ), IFN-γ, Granzyme B, NFAT5, and T-bet confirmed the robust T cell activation (Fig. 1A). A total of 3,619 and 4,708 differentially expressed genes (DEGs) were identified at 12 and 24 h post-stimulation, respectively (Fig. S1A, S1B), with the majority showing sustained upregulation (Fig. S1C). DEGs were significantly enriched in processes such as cell cycle regulation, intracellular signal transduction, response to cytokine stimulus, cell proliferation, and immune system processes (Fig. S1D-S1F). Notably, carbohydrate metabolic processes—including biosynthesis, transport, and glycolysis—were significantly enriched, along with mitochondrial-related metabolic pathways (Fig. 1B, S1G). Genes involved in glycolysis (e.g., pfkla, hk2, h6pd, tpi1a) and mitochondrial OXPHOS (e.g., cox4i2, Nrf-1) were also significantly upregulated (Fig. 1C, D). Further experiments reinforced these findings. Activated T cells demonstrated increased glucose uptake (Fig. 1E, F) and upregulated transcription of glycolysis-related genes, including glucose transporter 1 (Glut1), hexokinase 2 (HK2), phosphofructokinase (PFK), and pyruvate kinase (PKM) (Fig. 1G). Increased expression of Glut1, HK2, PFK and PKM, and enzyme activity of HK2 and PKM were also observed (Fig. 1H-J). Likewise, mitochondrial OXPHOS was also activated, for T cell stimulation led to the upregulation of OXPHOS-related genes, such as Ndufb3, Sdhb, and cytochrome c1 (Cyc1) (Fig. 1K, L). Overall, these results suggest that T cell activation in tilapia is strongly associated with both glycolysis and OXPHOS.

Tilapia utilizes PI3K-AKT-GSK3β axis to mediate T cell metabolism

Next, we aimed to elucidate the mechanisms by which tilapia T cells regulate metabolic programs. KEGG analysis revealed significant enrichment of several critical pathways for T cell immunity upon activation, including JAK-STAT, MAPK, AMPK, PI3K-AKT, and mTOR (Fig. 1M, S2 A). Notably, the PI3K-AKT signaling pathway and its downstream molecule GSK3β, vital for various metabolic processes, were consistently upregulated (Fig. 1N). Furthermore, GSK3β was predicted to interact with several molecules, such as AKT1, mTOR, and HK2, facilitating intracellular signal transduction (Fig. 1O). Approximately 35% of these target genes were implicated in metabolic programs (Fig. S2B, S2 C), indicating that GSK3β may play a pivotal role in T cell metabolism in tilapia. The GSK3β gene is located on chromosome LG16 of tilapia, forming an evolutionarily conserved gene cluster (Fig. S3 A). Tilapia GSK3β exhibits high similarity to its homologs in other vertebrates in terms of amino acid sequence, functional domains, and tertiary structure, particularly at the two phosphorylation sites, Ser9 and Tyr216 (Fig. S3B, S3 C). Phylogenetic analysis shows that tilapia GSK3β clusters closely with those from other teleost fish (Fig. S3D).

GSK3β is broadly expressed in immune-related tissues of tilapia (Fig. S4 A). Upon T cell activation, the mRNA levels of PI3K, AKT, and GSK3β were significantly upregulated (Fig. S4B). Simultaneously, the phosphorylation of AKT, GSK3β (Tyr216), and GSK3β (Ser9) were markedly increased (Fig. 1P). Treatment with the AKT inhibitor oridonin impaired the phosphorylation of GSK3β at both Tyr216 and Ser9 (Fig. 1Q). Additionally, AKT was found to directly interact with GSK3β (Fig. 1R), enhancing the transcriptional activity of the GSK3β promoter (Fig. 1S). These results suggest that tilapia employs the PI3K-AKT-GSK3β axis for T cell signal transduction. Given that T cell activation is linked to both metabolic reprogramming and GSK3β signaling, we further examined the relationship between GSK3β and metabolic pathways. Overexpression of tilapia GSK3β did not affect the phosphorylation of AKT or Erk1/2 (Fig. 1T); however, it decreased AMPK phosphorylation (Fig. 1T) while enhancing the phosphorylation of mTORC1, S6, and 4E-BP1, indicating the activation of

Fig. 1 Tilapia utilizes PI3K-AKT-GSK3β axis to mediate T cell metabolism. **A-D** Tilapia spleen lymphocytes stimulated with CD3/CD28 mAbs for 12 or 24 h were subjected to RNA-seq analysis, $n = 4$. (**A**, **C**, **D**) Heatmaps showing the genes related to T cell activation (**A**), glycolysis (**C**) and OXPHOS (**D**). **B** GO pathway enrichment analysis showing the top nine pathways in metabolism process. **E-L** Tilapia spleen lymphocytes were stimulated with CD3/CD28 mAbs for indicated time. **E**, **F** Histograms and bar figure showing the uptake of 2-NBDG in gated $CD3^+$ T cells at 12 h, $n = 3$. **G**, **K** Relative mRNA levels of indicated genes at 12 h, $n = 4$ or 6. **H**, **I**, **L** Western blot showing the protein levels of indicated molecules at indicated time points (**H**, **I**) or 3 h (**L**). **J** Enzyme activities of indicated molecules at 12 h, $n = 4$. **M** KEGG pathway enrichment analysis showing the top ten pathways in immunology at 24 h. **N** Heatmaps showing the genes related to T cell signaling pathway. **O** Protein–protein interaction analysis showing the predicted interaction networks of GSK3β. (**P**, **Q**) Tilapia spleen lymphocytes were stimulated with CD3/CD28 mAbs for indicated time. **P** Western blot showing the expression of indicated molecules. **Q** CD3/CD28 mAbs-stimulated lymphocytes were treated with AKT inhibitor oridonin or not. Western blot showing the expression of indicated molecules at 3 h. **R** Tilapia GSK3β and AKT were overexpressed in HEK 293 T cells. Co-IP assay showing the interaction between GSK3β and AKT. **S** HEK 293 T cells were co-transfected with GSK3β promoter and AKT, and GSK3β promoter activity was examined by dual-luciferase assay at 48 h post transfection, $n = 4$. **T-W** Tilapia GSK3β was overexpressed in HEK 293 T cells, and western blot showing the expression of indicated molecules. Experiments were repeated for three independent times. *: $p < 0.05$, **: $p < 0.01$, ***: $p < 0.001$, determined by a two-tailed Student's t test

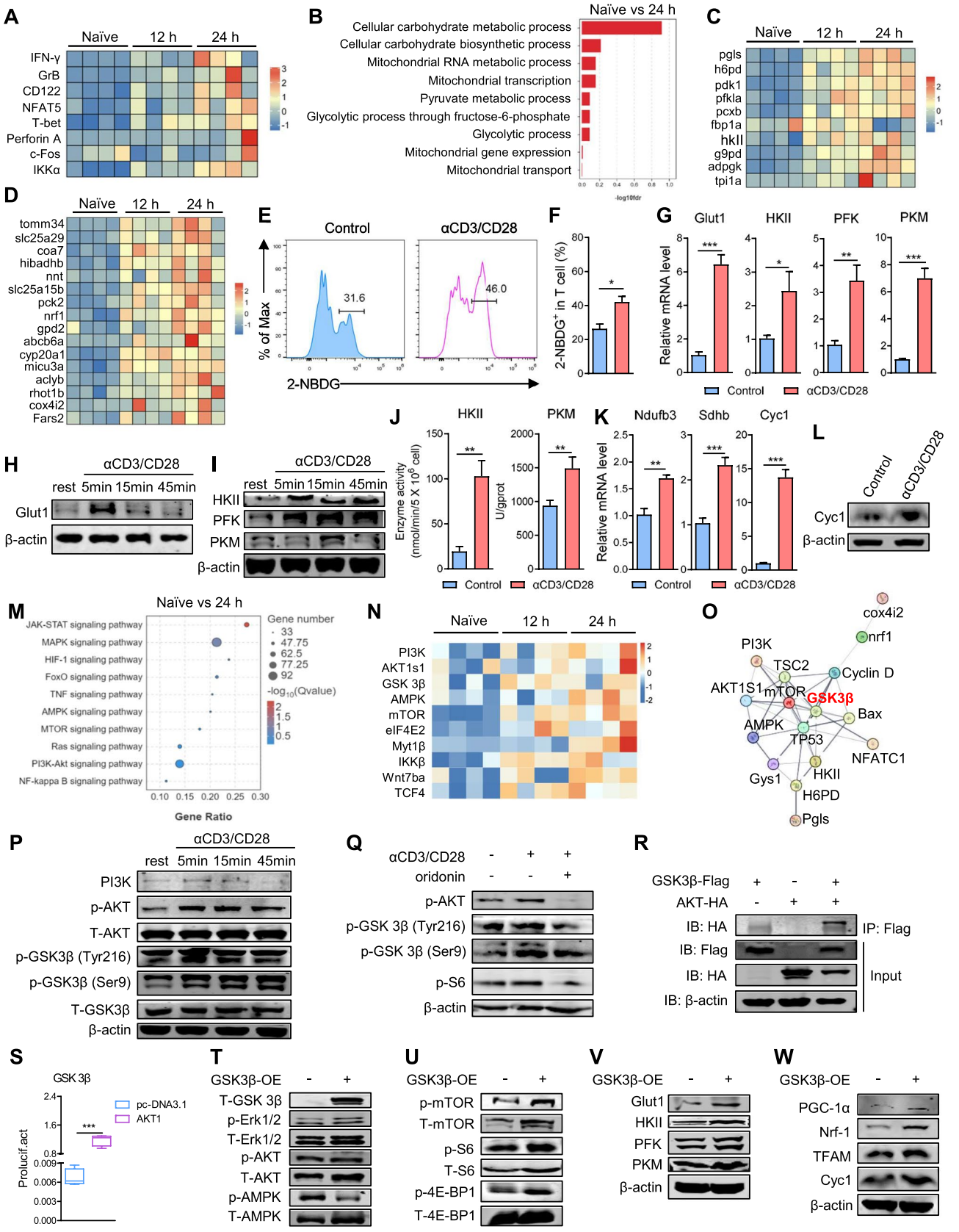
A
Naïve
12 h
24 h
IFN-γ
GrB
CD122
NFAT5
T-bet
Perforin A
c-Fos
IKKα
B
Naïve vs 24 h
Cellular carbohydrate metabolic process
Cellular carbohydrate biosynthetic process
Mitochondrial RNA metabolic process
Mitochondrial transcription
Pyruvate metabolic process
Glycolytic process through fructose-6-phosphate
Glycolytic process
Mitochondrial gene expression
Mitochondrial transport
C
Naïve
12 h
24 h
pgls
h6pd
pdk1
pfkla
pcxb
fbp1a
hkII
g9pd
adpgk
tpi1a
D
Naïve
12 h
24 h
tomm34
slc25a29
coa7
hibadhb
nnt
slc25a15b
pck2
nrf1
gpd2
abcb6a
cyp20a1
micu3a
aclyb
rhot1b
cox4i2
Fars2
E
Control
αCD3/CD28
% of Max
31.6
46.0
2-NBDG
F
2-NBDG+ in T cell (%)
G
Glut1
HKII
PFK
PKM
Relative mRNA level
Control
αCD3/CD28
H
αCD3/CD28
rest 5min 15min 45min
Glut1
β-actin
I
αCD3/CD28
rest 5min 15min 45min
HKII
PFK
PKM
β-actin
J
HKII
PKM
Enzyme activity (nmol/min/5 X 10^6 cell)
U/gprot
Control
αCD3/CD28
K
Ndufb3
Sdhb
Cyc1
Relative mRNA level
Control
αCD3/CD28
L
Control
αCD3/CD28
Cyc1
β-actin
M
Naïve vs 24 h
JAK-STAT signaling pathway
MAPK signaling pathway
HIF-1 signaling pathway
FoxO signaling pathway
TNF signaling pathway
AMPK signaling pathway
MTOR signaling pathway
Ras signaling pathway
PI3K-Akt signaling pathway
NF-kappa B signaling pathway
Gene number
-log10(Qvalue)
Gene Ratio
N
Naïve
12 h
24 h
PI3K
AKT1s1
GSK 3β
AMPK
mTOR
eIF4E2
Myt1β
IKKβ
Wnt7ba
TCF4
O
cox4i2
nrf1
PI3K
TSC2
Cyclin D
AKT1S1
mTOR
GSK3β
Bax
AMPK
TP53
NFATC1
Gys1
HKII
H6PD
Pgls
P
αCD3/CD28
rest 5min 15min 45min
PI3K
p-AKT
T-AKT
p-GSK3β (Tyr216)
p-GSK3β (Ser9)
T-GSK3β
β-actin
Q
αCD3/CD28 - + +
oridonin - - +
p-AKT
p-GSK 3β (Tyr216)
p-GSK 3β (Ser9)
p-S6
β-actin
R
GSK3β-Flag + - +
AKT-HA - + +
IB: HA
IB: Flag
IB: HA
IB: β-actin
IP: Flag
Input
S
GSK 3β
pc-DNA3.1
AKT1
Prolucif.act
T
GSK3β-OE - +
T-GSK 3β
p-Erk1/2
T-Erk1/2
p-AKT
T-AKT
p-AMPK
T-AMPK
U
GSK3β-OE - +
p-mTOR
T-mTOR
p-S6
T-S6
p-4E-BP1
T-4E-BP1
V
GSK3β-OE - +
Glut1
HKII
PFK
PKM
β-actin
W
GSK3β-OE - +
PGC-1α
Nrf-1
TFAM
Cyc1
β-actin

mTORC1 pathway (Fig. 1U). Notably, GSK3β overexpression increased the expression of glycolytic enzymes such as Glut1, HKII, PFK, and PKM (Fig. 1V) and elevated the levels of proteins involved in OXPHOS, including PGC-1α, Nrf-1, TFAM, and Cyc1 (Fig. 1W). Altogether, these findings suggest that GSK3β signaling may regulate both glycolysis and OXPHOS in tilapia.

GSK3β promotes tilapia T cell glycolysis through Tyr216 phosphorylation

Then, we investigated the regulatory role of GSK3β in T cell metabolism. The GSK3β inhibitor Chir effectively suppressed activation-induced phosphorylation of GSK3β at Tyr216 (Fig. 2A), leading to reduced glucose uptake in $CD3^+$ T cells (Fig. 2B). Inhibiting Tyr216 phosphorylation also impaired the upregulation of glycolysis-related enzymes HK2, PFK, and PKM at both mRNA and protein levels (Fig. 2C, S4 C), and reduced the activity of HK2 and PKM (Fig. 2D), indicating that GSK3β promotes glycolysis in tilapia T cells via Tyr216 phosphorylation. In contrast, Chir administration did not affect the expression of key OXPHOS components such as PGC-1α, Nrf-1, TFAM, and Cyc1 (Fig. 2E), suggesting that Tyr216 phosphorylation is not essential for OXPHOS in tilapia T cells. Notably, blocking Tyr216 phosphorylation impaired T cell activation, as shown by the decreased S6, 4EBP1 and ERK1/2 phosphorylation (Fig. 2F, G) and the impaired CD122, CD44 and IFN-γ expression (Fig. 2H). Meanwhile, the activation-induced apoptosis of $CD3^+$ T cells was also increased upon Chir treatment (Fig. 2I). Overall, our findings suggest that phosphorylation of GSK3β at Tyr216 links glycolysis, rather than OXPHOS, to enhance T cell activation and survival in tilapia.

Tyr216 phosphorylation-driven glycolysis is crucial for the T cell immunity in tilapia

Since Tyr216 phosphorylation of GSK3β regulates the T cell activation, we further investigated its effect on anti-bacterial immunity of tilapia. Consistent with previous reports, T cells in spleen were dramatically increased after *E. piscicida* infection [28]. However, blocking Tyr216 phosphorylation significantly reduced the proportion and number of T cells (Fig. 2J, K). This reduction was associated with impaired T cell activation and proliferation, as well as increased apoptosis. Because blocking GSK3β Tyr216 phosphorylation during *E. piscicida* infection dampened the phosphorylation of AKT, mTOR, S6, 4EBP1 and ERK1/2 that are crucial for T cell activation (Fig. 2L), reduced the proportion of $CD3\varepsilon^+$ $BrdU^+$ cells (Fig. 2M, N), and elevated the apoptosis of $CD3\varepsilon^+$ T cells (Fig. 2O, P). Furthermore, deficiency of Tyr216 phosphorylation impaired the inducible expression of cytotoxic genes such as perforin A, IFN-γ and TNF-α (Fig. 2Q), which ultimately crippled the ability of tilapia to clear pathogen infection (Fig. 2R). These results support that phosphorylation of GSK3β at Tyr216 is essential for proper T cell response to resist bacterial infection. Notably, this compromised T cell immunity induced by Tyr216 phosphorylation deprivation was accompanied by a decreased glycolysis level, as evidenced by the impaired mRNA or protein level of Glut1, HK2, PFK and PKM (Fig. 2S, S4D). These findings thus suggest that phosphorylation of GSK3β at Tyr216 may orchestrate the T cell response during bacterial infection via promoting glycolysis.

Fig. 2 Tyr216 phosphorylation-driven glycolysis is essential for the T cell immunity in tilapia. **A**-**I** Tilapia spleen lymphocytes were stimulated with CD3/CD28 mAbs in the presence or absence of the inhibitor Chir99021 for indicated time points. **A**, **C**, **E**, **F** Western blot showing the expression of indicate molecules at 3 h. **B** Histograms showing the uptake of 2-NBDG in gated $CD3^+$ T cells at 3 h. **D** Bar figures showing the enzyme activities at 12 h, $n = 4$–6. **G** Histograms showing the phosphorylation level of Erk1/2 in gated $CD3^+$ T cells at 12 h. **H** Relative mRNA levels of indicated genes at 12 h, $n = 4$–6. **I** FACS plots showing the Annexin V and 7-AAD staining in gated $CD3^+$ T cells at 12 h. **J**-**S** Tilapia individuals that infected with *E. piscicida* were injected with the inhibitor Chir99021, and spleen lymphocytes were harvested at indicated days for assay. **J**, **K** FACS plots and bar figure showing the T cell percentage and number in spleen at 4 or 7 dpi, $n = 4$–6. **L**, **S** Western blot showing the expression levels of indicated molecules at 4 dpi. **M**, **N** FACS plots and bar figure showing the BrdU incorporation in $CD3^+$ T cells at 4 dpi, $n = 4$. **O**, **P** FACS plots and bar figure showing the Annexin V and 7-AAD staining in gated $CD3^+$ T cells at 4 dpi, $n = 3$ or 4. **Q** Relative mRNA levels of indicated molecules were examined by qPCR, $n = 4$ or 6. **R** Bacterial titer in liver at 5 dpi, $n = 4$. All the experiments were repeated for three independent times. *: $p < 0.05$, **: $p < 0.01$, ***: $p < 0.001$, determined by a two-tailed Student's t test

Glycolysis is essential for the proper activation of T cells in tilapia

The metabolic shift from FAO to glycolysis plays a pivotal role in regulating T cell activation in mammals [35]. However, from a nutritional perspective, fish exhibit significantly lower requirements for glucose compared to mammals [36]. This raises an important question: to what extent does T cell response in fish depend on glycolysis? We found that mRNA levels of Glut1 and PKM in lymphocytes were increased upon T cell activation, while this inducible expression was markedly weakened once glucose was deprived (Fig. 3A). The same was also true for the protein levels (Fig. 3B). Moreover, depriving glucose impaired the T cell activation in tilapia, as revealed by the reduced S6 and Erk1/2 phosphorylation (Fig. 3C, D) and CD122 and IFN-γ transcription (Fig. 3E). These results indicate a potential involvement of glycolysis in the T cell activation of tilapia. To confirm whether the dependence of T cell activation on glucose is attributed to glycolysis, the HK2 inhibitor

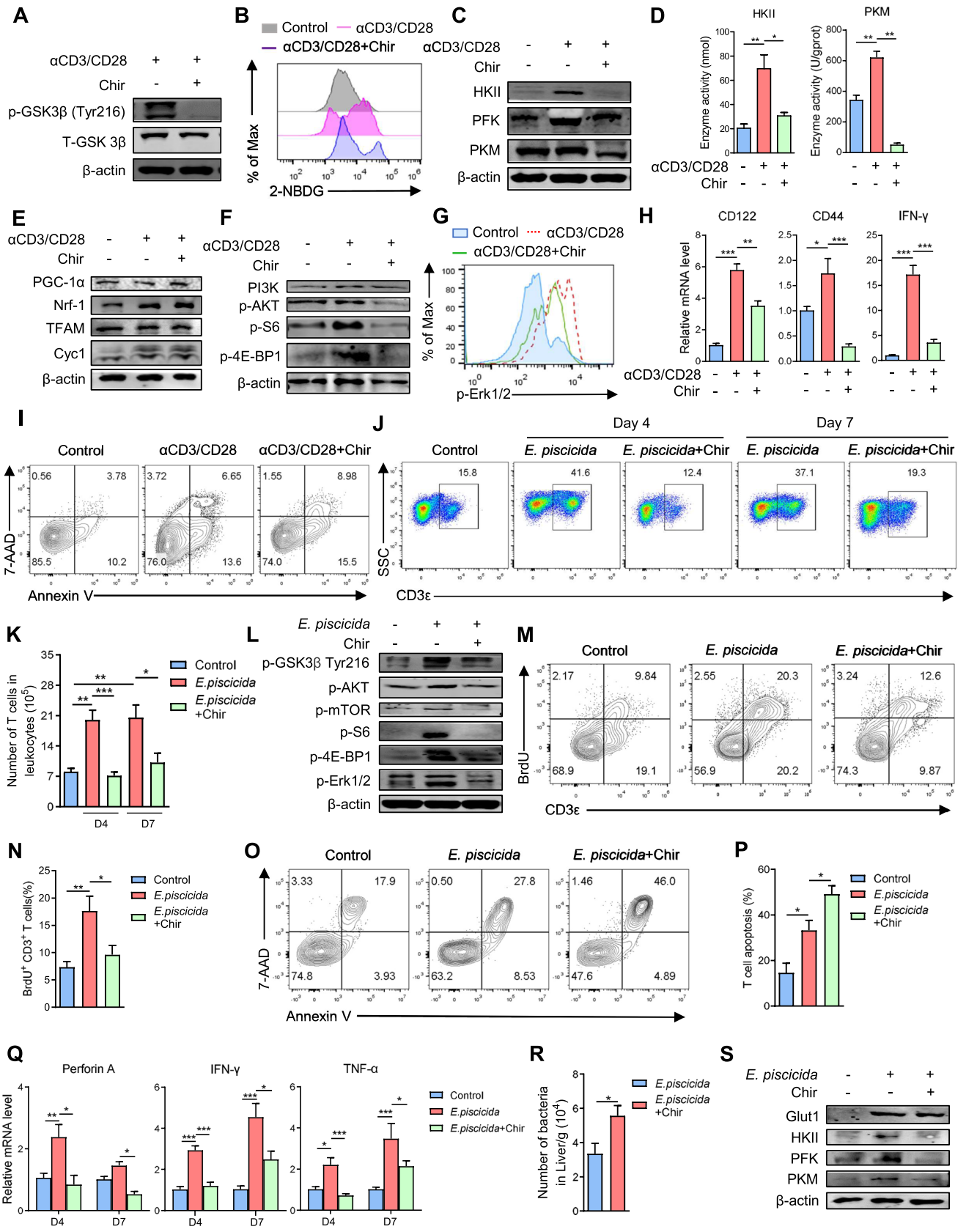
A
αCD3/CD28
Chir
p-GSK3β (Tyr216)
T-GSK 3β
β-actin
B
Control
αCD3/CD28
αCD3/CD28+Chir
% of Max
2-NBDG
C
αCD3/CD28
Chir
HKII
PFK
PKM
β-actin
D
HKII
PKM
Enzyme activity (nmol)
Enzyme activity (U/gprot)
αCD3/CD28
Chir
E
αCD3/CD28
Chir
PGC-1α
Nrf-1
TFAM
Cyc1
β-actin
F
αCD3/CD28
Chir
PI3K
p-AKT
p-S6
p-4E-BP1
β-actin
G
Control
αCD3/CD28
αCD3/CD28+Chir
% of Max
p-Erk1/2
H
CD122
CD44
IFN-γ
Relative mRNA level
αCD3/CD28
Chir
I
Control
αCD3/CD28
αCD3/CD28+Chir
7-AAD
Annexin V
0.56
3.78
85.5
10.2
3.72
6.65
76.0
13.6
1.55
8.98
74.0
15.5
J
Day 4
Day 7
Control
E. piscicida
E. piscicida+Chir
E. piscicida
E. piscicida+Chir
SSC
CD3ε
15.8
41.6
12.4
37.1
19.3
K
Number of T cells in leukocytes (10^5)
Control
E.piscicida
E.piscicida +Chir
D4
D7
L
E. piscicida
Chir
p-GSK3β Tyr216
p-AKT
p-mTOR
p-S6
p-4E-BP1
p-Erk1/2
β-actin
M
Control
E. piscicida
E. piscicida+Chir
BrdU
CD3ε
2.17
9.84
68.9
19.1
2.55
20.3
56.9
20.2
3.24
12.6
74.3
9.87
N
BrdU+ CD3+ T cells(%)
Control
E.piscicida
E.piscicida +Chir
O
Control
E. piscicida
E. piscicida+Chir
7-AAD
Annexin V
3.33
17.9
74.8
3.93
0.50
27.8
63.2
8.53
1.46
46.0
47.6
4.89
P
T cell apoptosis (%)
Control
E.piscicida
E.piscicida +Chir
Q
Perforin A
IFN-γ
TNF-α
Relative mRNA level
Control
E.piscicida
E.piscicida+Chir
D4
D7
R
Number of bacteria in Liver/g (10^4)
E.piscicida
E.piscicida +Chir
S
E. piscicida
Chir
Glut1
HKII
PFK
PKM
β-actin

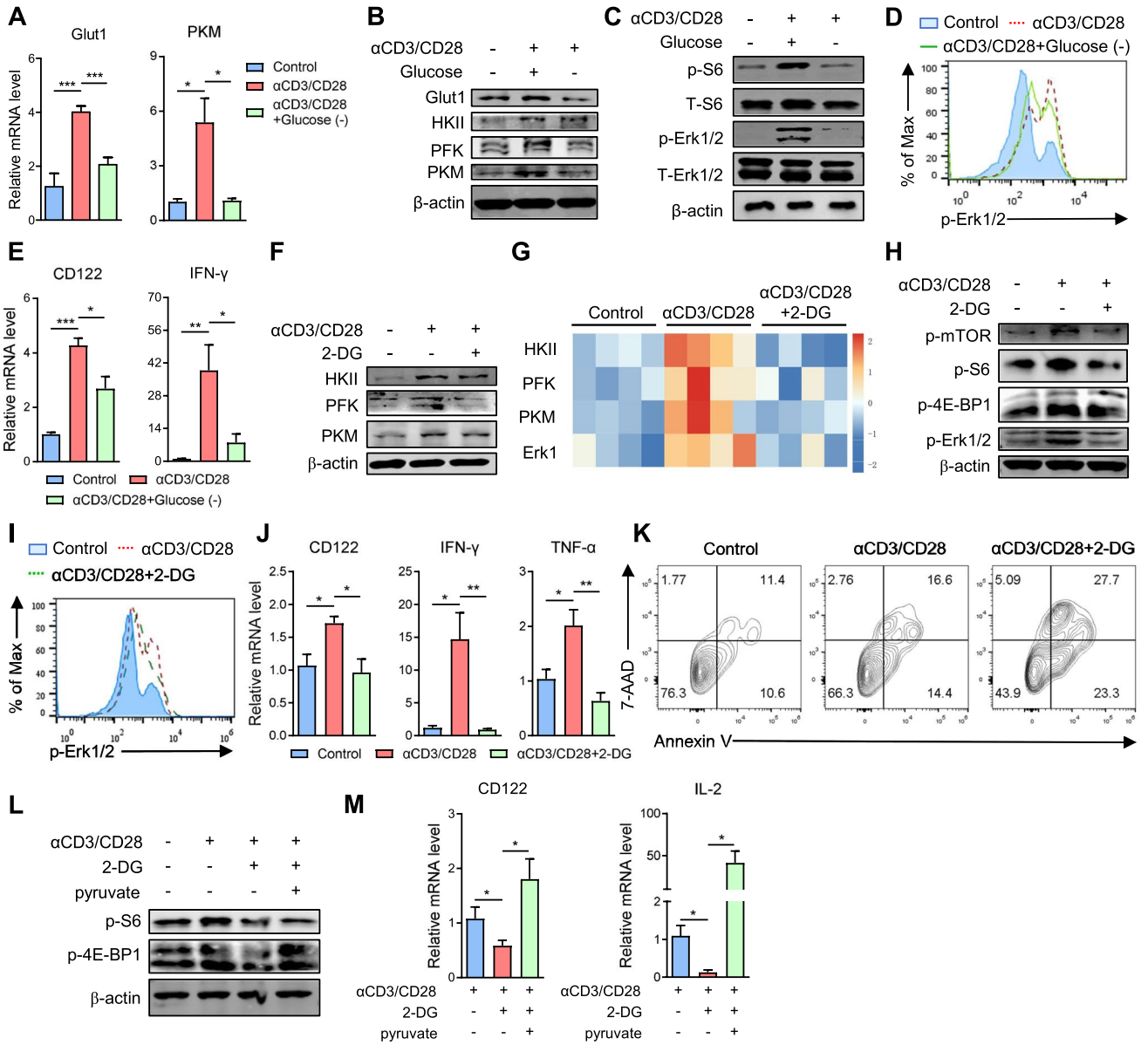

Fig. 3 Glycolysis is pivotal for T cell activation in tilapia. **A**-**E** Tilapia spleen lymphocytes were stimulated with CD3/CD28 mAbs in the presence or absence of glucose. **A**, **E** Relative mRNA levels of indicated molecules were examined by qPCR at 12 h, $n = 4$ or 5. **B**, **C** Western blot showing the expression levels of indicated molecules at 3 h. **D** Histograms showing the phosphorylation level of Erk1/2 in gated $CD3^+$ T cells at 12 h. **F**-**K** Tilapia spleen lymphocytes were stimulated with CD3/CD28 mAbs in the presence or absence of the inhibitor 2-DG for indicated time points. **F**, **H** Western blot showing the expression levels of indicated molecules at 3 h. **G** Heatmap showing the relative mRNA levels of indicated genes examined by qPCR at 12 h, $n = 4$. **I** Histograms showing the phosphorylation level of Erk1/2 in gated $CD3^+$ T cells at 12 h. **J** Relative mRNA levels of indicated molecules were examined by qPCR at 12 h, $n = 4$ or 6. **K** FACS plots showing the Annexin V and 7-AAD staining in gated $CD3^+$ T cells at 12 h. **L**, **M** CD3/CD28 mAbs-stimulated tilapia spleen lymphocytes were treated with inhibitor 2-DG in the presence or absence of pyruvate. **L** Western blot showing the expression levels of indicated molecules at 3 h. **M** Relative mRNA levels of indicated molecules examined by qPCR at 12 h, $n = 4$. All the experiments were repeated for three independent times. *: $p < 0.05$, **: $p < 0.01$, ***: $p < 0.001$, determined by a two-tailed Student's t test

2-DG was employed to suppress glycolysis. During the CD3/CD28 mAb-induced T cell activation, 2-DG administration impaired the up-regulation of HK2, PFK, and PKM at both mRNA and protein levels (Fig. 3F, G), indicating an inhibited glycolysis. Notably, the inducible phosphorylation of mTOR, S6, 4EBP1 and ERK1/2 in spleen lymphocytes (Fig. 3H) or phosphorylation of ERK1/2 in gated $CD3^+$ T cells (Fig. 3I), and inducible expression of CD122, IFN-γ and TNF-α (Fig. 3J), were coincidently inhibited upon 2-DG administration, suggesting glycolysis may be essential for the activation of T cells in tilapia. In addition, inhibition of glycolysis exacerbated the activation-induced T cell

apoptosis (Fig. 3K). To confirm the impaired T cell activation in tilapia was indeed caused by the defective glycolysis, pyruvate, a metabolite of glycolysis was used to rescue the defective T cell response. Upon glycolysis inhibition, addition of additional pyruvate fully rescued the dampened S6 and 4EBP1 phosphorylation (Fig. 3L) and CD122 and IL-2 expression (Fig. 3M). Overall, these findings suggest that glycolysis is essential for the proper activation of T cells in tilapia.

Activating GSK3β by inhibiting Ser9 phosphorylation enhances T cell response via OXPHOS in tilapia

Because T cell activation, as well as GSK3β overexpression, induced both glycolysis and OXPHOS, whereas Tyr216 phosphorylation regulates glycolysis only, we hypothesized that the OXPHOS in tilapia T cells was controlled by the Ser9 phosphorylation of GSK3β. Ser9 phosphorylation inactivates GSK3β function, while inhibition of its phosphorylation can promote [37–39]. Administration of the inhibitor SB216763 (SB) could block the T cell activation-induced GSK3β phosphorylation at Ser9 (Fig. 4A). Unlike Tyr216, inhibition of Ser9 phosphorylation did not affect glycolysis (Fig. 4B). However, upon T cell activation, activating GSK3β by blocking Ser9 phosphorylation further elevated the mRNA and protein levels of Cyc1, as well as the evolutionarily conserved PGC-1α/Nrf-1/TFAM axis (Fig. 4C-E and Fig. S5-S7), which play crucial roles in regulating OXPHOS in mammals [40], suggesting an enhanced OXPHOS. This increased OXPHOS was also observed during *E. piscicida* infection (Fig. 4F). Notably, inhibition of Ser9 phosphorylation further promoted the T cell activation, revealing by the increased Erk1/2 phosphorylation and the CD122 and IL-2 expression (Fig. 4G, 4H), and alleviated the activation-induced T cell apoptosis (Fig. 4I, J). The reduced apoptosis in T cells lacking Ser9 phosphorylation may benefit from the higher mitochondrial membrane potential (Fig. 4K) and lower reactive oxygen species (ROS) level (Fig. 4L, M). Furthermore, activating GSK3β by inhibiting Ser9 phosphorylation promoted T cell activation and survival during *E. piscicida* infection (Fig. 4N, O), and further amplified T cell capacity to produce pro-inflammatory cytokines and cytotoxic molecules (Fig. 4P), ultimately accelerating pathogen clearance (Fig. 4Q) and improving tilapia survival (Fig. 4R). These findings suggest that activating GSK3β by inhibiting Ser9 phosphorylation can regulate T cell response via OXPHOS.

OXPHOS is essential for tilapia T cell immunity

Considering inhibiting Ser9 phosphorylation of GSK3β promote T cell immunity while enhancing OXPHOS in tilapia, we further sought to investigate the association between OXPHOS and T cell response. Antimycin A, an inhibitor of mitochondrial respiratory chain was used to treat tilapia leukocytes. Antimycin A did not affect T cell activation-induced glycolysis (Fig. 5A), but impaired the up-regulation of Cyc1 after αCD3/CD28 mAb stimulation (Fig. 5B), and reduced the transcription levels of another two respiratory chain complexes, Ndufb3 and Sdhb (Fig. 5C), indicating that Antimycin A inhibited the OXPHOS in tilapia T cells. Meanwhile, blocking OXPHOS impaired the activation of MAPK/ERK and mTORC1 signaling and compromised the inducible expressions of CD122 and IFN-γ during T cell activation (Fig. 5D, E), and also regulated the AKT-GSK3β axis in a feedback manner (Fig. 5F). This suggests that OXPHOS is essential for the T cell activation in tilapia. Moreover, inhibition of OXPHOS reduced the expression of c-Myc (Fig. 5G), a transcription factor crucial for cellular proliferation, and resulted in a defective T cell proliferation (Fig. 5H), and exacerbated the T cell apoptosis (Fig. 5I). Intriguingly, inhibiting OXPHOS with Antimycin A also impaired the inducible expression of PGC-1α/Nrf-1/TFAM axis during T cell activation (Fig. 5J, K), suggesting that tilapia utilizes the feedback regulatory mechanism between PGC-1α/Nrf-1/TFAM axis and OXPHOS to stabilize their regulation on T cell immunity. Therefore, our results support a notion that OXPHOS is required for the proper T cell immunity in tilapia.

GSK3β Tyr216 phosphorylation orchestrates both glycolysis and OXPHOS to promote $CD4^+$ and $CD8^+$ T cell immunity in mouse

Since the two phosphorylation sites of GSK3β differentially link to glycolysis and OXPHOS, thereby promoting T cell immunity in bony fish, we aim to further investigate whether similar mechanisms exist in mouse. Upon CD3/CD28 mAb activation, Tyr216 phosphorylation of GSK3β was inhibited by Chir in mouse splenocytes (Fig. 6A). Similar to that in tilapia, inhibition of Tyr216 phosphorylation compromised the glycolysis induced by T cell activation (Fig. 6B). However, the OXPHOS was impaired synchronously (Fig. 6C), suggesting unlike that in fish, Tyr216 phosphorylation of GSK3β promotes both glycolysis and OXPHOS in mouse T cells. Similarly, blocking Tyr216 phosphorylation impaired the CD3/CD28 mAbs-induced T cell activation, as revealed by the decreased phosphorylation of Erk1/2 and mTORC1 signals (Fig. 6D), and down-regulated CD69 expression in $CD4^+$ T cells and $CD8^+$ T cells (Fig. 6E, F). Moreover, $CD4^+$

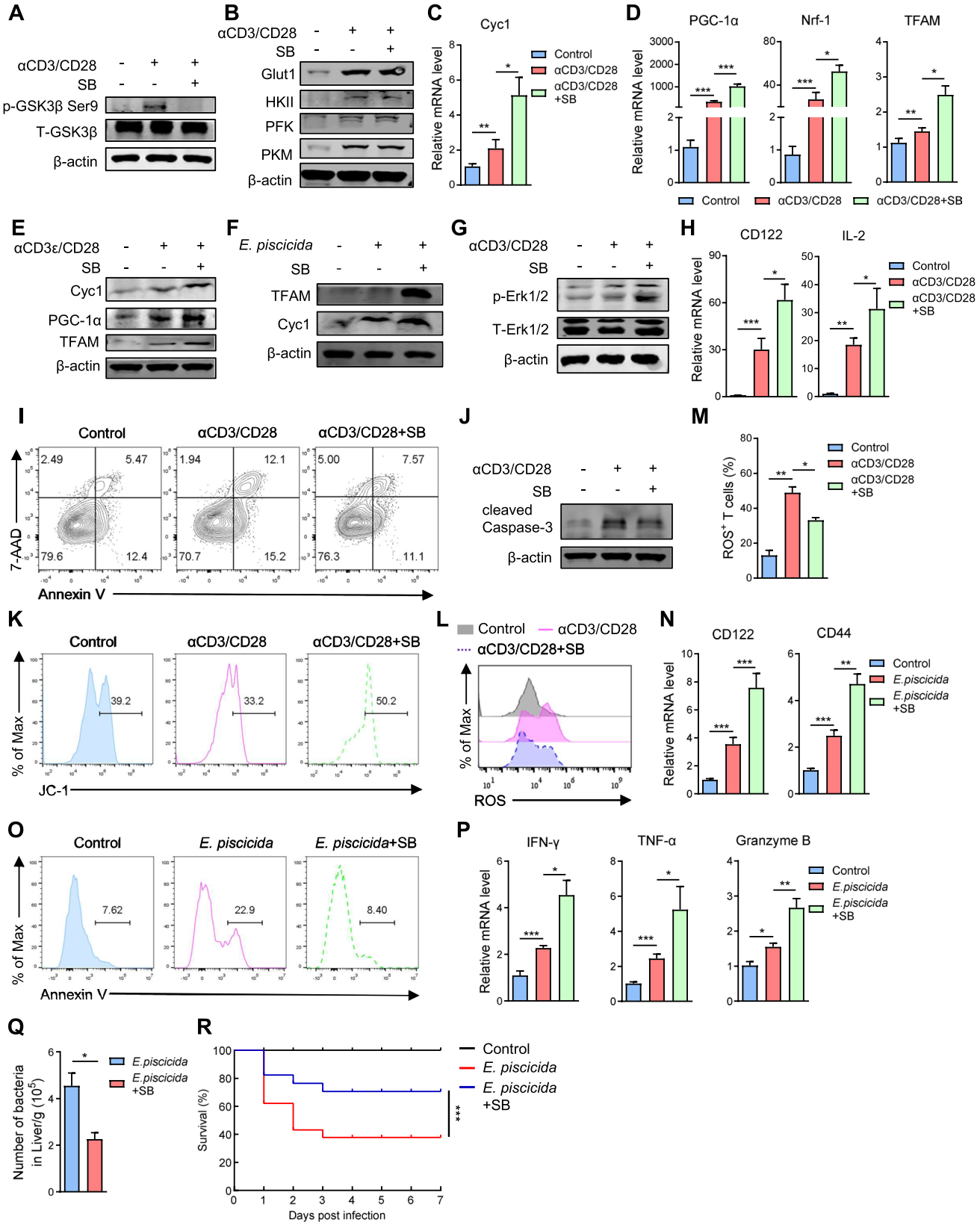
A
αCD3/CD28 - + +
SB - - +
p-GSK3β Ser9
T-GSK3β
β-actin
B
αCD3/CD28 - + +
SB - - +
Glut1
HKII
PFK
PKM
β-actin
C
Cyc1
Relative mRNA level
Control
αCD3/CD28
αCD3/CD28 +SB
D
PGC-1α
Nrf-1
TFAM
Relative mRNA level
Control
αCD3/CD28
αCD3/CD28+SB
E
αCD3ε/CD28 - + +
SB - - +
Cyc1
PGC-1α
TFAM
β-actin
F
E. piscicida - + +
SB - - +
TFAM
Cyc1
β-actin
G
αCD3/CD28 - + +
SB - - +
p-Erk1/2
T-Erk1/2
β-actin
H
CD122
IL-2
Relative mRNA level
Control
αCD3/CD28
αCD3/CD28 +SB
I
Control
αCD3/CD28
αCD3/CD28+SB
2.49 5.47 79.6 12.4
1.94 12.1 70.7 15.2
5.00 7.57 76.3 11.1
7-AAD
Annexin V
J
αCD3/CD28 - + +
SB - - +
cleaved Caspase-3
β-actin
M
ROS+ T cells (%)
Control
αCD3/CD28
αCD3/CD28 +SB
K
Control
αCD3/CD28
αCD3/CD28+SB
39.2
33.2
50.2
% of Max
JC-1
L
Control
αCD3/CD28
αCD3/CD28+SB
% of Max
ROS
N
CD122
CD44
Relative mRNA level
Control
E.piscicida
E.piscicida +SB
O
Control
E. piscicida
E. piscicida+SB
7.62
22.9
8.40
% of Max
Annexin V
P
IFN-γ
TNF-α
Granzyme B
Relative mRNA level
Control
E.piscicida
E.piscicida +SB
Q
Number of bacteria in Liver/g (10^5)
E.piscicida
E.piscicida +SB
R
Survival (%)
Days post infection
Control
E. piscicida
E. piscicida +SB

Fig. 4 Inhibition of Ser9 phosphorylation enhances T cell response via OXPHOS in tilapia. **A-E**, **G-M** Tilapia spleen lymphocytes were stimulated with CD3/CD28 mAbs in the presence or absence of the inhibitor SB216763 for indicated time points. **A**, **B**, **E**, **G**, **J** Western blot showing the expression levels of indicated molecules at 3 h (**A**, **E**, **J**) or 6 h (**B**, **G**). **C**, **D**, **H** Relative mRNA levels of indicated molecules were examined by qPCR at 12 h, $n = 4$ or 6. **I** FACS plots showing the Annexin V and 7-AAD staining in gated $CD3^+$ T cells at 12 h. **K** Histograms showing the mitochondrial potential in gated $CD3^+$ T cells at 12 h. **L**, **M** Histograms and bar figure showing the ROS levels in gated $CD3^+$ T cells at 12 h, $n = 3$. **F**, **N-R** Tilapia individuals that infected with *E. piscicida* were injected with the inhibitor SB216763, and spleen lymphocytes were harvested at indicated days for assay. **F** Western blot showing the expression levels of indicated molecules at 4 dpi. **O** Histograms showing the Annexin V staining in gated $CD3^+$ T cells at 5 dpi. **P** Relative mRNA levels of indicated molecules were examined by qPCR at 5 dpi, $n = 4$ or 6. **Q** Bacterial titer in liver at 5 dpi, $n = 4$. **R** The survival curve of tilapia during bacterial infection, $n \geq 17$. All the experiments were repeated for three independent times. *: $p < 0.05$, **: $p < 0.01$, ***: $p < 0.001$, determined by a two-tailed Student's t test

T cells and $CD8^+$ T cells lacking GSK3β Tyr216 phosphorylation were failed to proliferate (Fig. 6G, H), which might be caused by the impaired IL-2 production (Fig. 6I, J and Fig. S8 A, S8B). Notably, Tyr216 phosphorylation is also essential for T cell function in mouse, because its suppression reduced the ability of $CD4^+$ T and $CD8^+$ T cells to produce IFN-γ (Fig. 6K, L and Fig. S8 C, S8D) and TNF-α (Fig. 6M, N and Fig. S8E, S8 F). These findings suggest that unlike coordinating glycolysis only in fish, phosphorylation of GSK3β at Tyr216 couples both glycolysis and OXPHOS to promote the $CD4^+$ and $CD8^+$ T cell response in mouse.

Inhibiting Ser9 phosphorylation restrains $CD4^+$ T cell activation and proliferation via suppressing OXPHOS in mouse

Finally, we investigated the regulation of GSK3β Ser9 phosphorylation on T cell glycolysis, OXPHOS, and immune response in mouse. Consist with tilapia, treatment with the inhibitor SB suppressed Ser9 phosphorylation in activated T cells of mouse (Fig. 7A), and had little effect on glycolysis (Fig. 7B). Interestingly, the higher GSK3β activity by inhibiting Ser9 phosphorylation did not enhance the OXPHOS as observed in tilapia, but weakened it (Fig. 7C); and further impaired the T cell activation (Fig. 7D-F), proliferation (Fig. 7G, H), and IL-2 production (Fig. 7I, J). However, inhibition of Ser9 phosphorylation weakened the production of IFN-γ in $CD4^+$ T cells (Fig. 7K and Fig. S8 C), but not IFN-γ in $CD8^+$ T cells (Fig. 7L and Fig. S8D) and TNF-α (Fig. 7M, N and Fig. S8E, S8 F). Overall, these findings suggest that activating GSK3β by inhibiting Ser9 phosphorylation restrains $CD4^+$ T cell activation and proliferation of mouse via suppressing OXPHOS.

Discussion

T cells undergo metabolic rewiring to fulfill the requirement of their activation, differentiation and function [41]. To establish the inherent correlation between T cell metabolism and phenotype, metabolic enzymes are indispensable. This study unravels how GSK3β mediates potential regulation of T cell immunity through distinct metabolic pathways. Additionally, we demonstrate that GSK3β reshaped metabolic strategies to regulate T cell immunity in vertebrates. These findings offer profound insights into how metabolic programs drive T cell function and immune plasticity.

Studies in mammals have shown the involvement of GSK3β in multiple cellular processes, including proliferation, apoptosis, DNA repair, cell cycle, and metabolism [42]. However, the role of GSK3β in apoptosis are not consistent. In mouse mesenchymal cells, GSK3β promoted Etoposide-induced apoptosis by activating caspase-3 and downregulating Bcl-2 [43]. Conversely, GSK3β also activated NF-κB pathway for Bcl-2 expression and protection from apoptosis [44, 45]. We demonstrated that phosphorylation of two distinct sites on GSK3β had opposing efficacy on T cell apoptosis in tilapia, highlighting the flexibility of GSK3β regulation on cell survival. This may partially explain the conflicting findings in mammals. GSK3β was found to regulate the innate immune response in bony fish, because during in vitro viral infection of spleen cells from *Epinephelus coioides*, GSK3β overexpression promoted Singapore grouper iridovirus (SGIV) replication and dramatically downregulated IFN-β, IFN-stimulated response elements, and NF-κB activity [46]. For the first time, our results emphasize, the role of GSK3β in regulating T cell immune response in fish, since inhibition of Tyr216 phosphorylation impaired, but blockade of Ser9 phosphorylation enhanced T cell mediated anti-bacterial immunity.

Despite GSK3β is known to control cellular metabolism and T cell response, whether it intimately decides T cell immunity via manipulating metabolic program remains unknown. For the first time, we proposed that GSK3β is a central hub linking T cell metabolism and immunity, in both fish and mouse. Studying the T cell metabolic reprogramming by GSK3β in lower vertebrates can provide important insights into the evolution of metabolic remodeling in immune cells. There have been few investigations related to the regulation of metabolism by GSK3β in bony fish, which are predominantly linked to lipid metabolism. For instance, the GSK3β/β-catenin pathway in *Larimichthys crocea* might regulate lipoprotein lipase and fatty acid synthase via peroxisome proliferator-activated receptor gamma (PPARγ), thereby modulating liver lipid deposition [31]. In addition, *Pelteobagrus fulvidraco* regulated phosphorus overload-induced lipolysis via GSK3β-PPARα axis [47]. However,

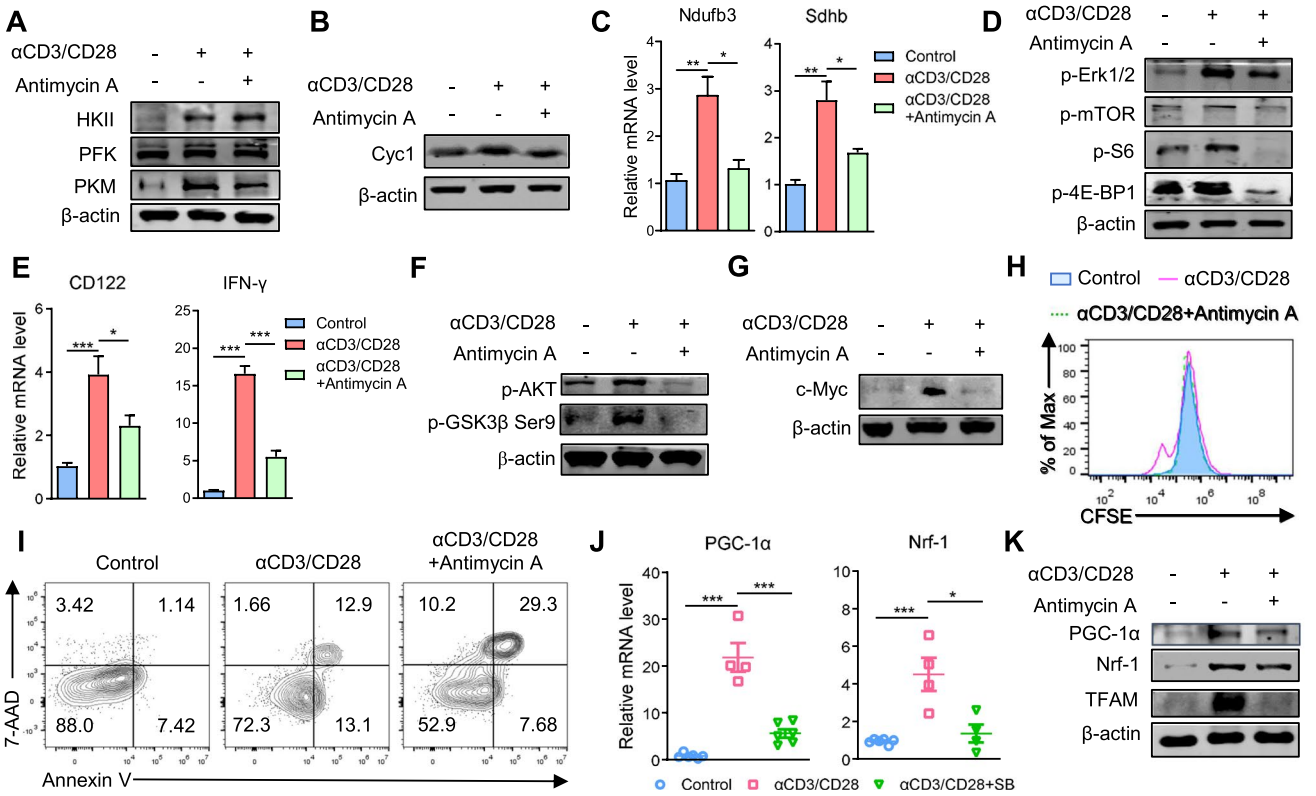

Fig. 5 OXPHOS promotes T cell immunity in tilapia. **A**-**K** Tilapia spleen lymphocytes were stimulated with CD3/CD28 mAbs in the presence or absence of the inhibitor Antimycin A for indicated time points. **A**, **B**, **D**, **F**, **G**, **K** Western blot showing the expression levels of indicated molecules at 3 h (**A**, **B**, **G**, **K**) or 6 h (**D**, **F**). **C**, **E**, **J** Relative mRNA levels of indicated molecules were examined by qPCR at 12 h, $n = 4$ or 6. **H** Tilapia spleen lymphocytes were labelled with CFSE and stimulated with CD3/CD28 mAbs. Histogram showing the proliferation of gated $CD3^+$ T cells at 48 h. (**I**) FACS plots showing the Annexin V and 7-AAD staining in gated $CD3^+$ T cells at 12 h. All the experiments were repeated for three independent times. *: $p < 0.05$, **: $p < 0.01$, ***: $p < 0.001$, determined by a two-tailed Student's t test

in fish, the lowest vertebrates possessing T cells, it remains unclear whether and how GSK3β coordinates metabolism to control T cell immunity. Upon T cell activation, TCR-mediated signals induce both glycolysis and mitochondrial metabolism. ATP production and calcium-dependent ROS increase, resulting from mitochondrial metabolism, are essential for complete T cell activation [48, 49]. T cell activation in tilapia induces the phosphorylation of GSK3β at Tyr216 and Ser9, leading to an enhanced glycolysis and OXPHOS. This suggests a dynamic adjustment of phosphorylation, specifically the timely dephosphorylation of the Ser9 site to enhance OXPHOS, thus supporting tilapia T cell activation. Notably, the in vitro culture environment differs from the in vivo microenvironment, so in vivo experiments are more proper to uncover the precise mechanisms that tilapia GSK3β dynamically regulates T cell immunity via dual-site phosphorylation-coupled metabolism. Future investigation will likely involve GSK3β gene knockout or site-directed mutagenesis using CRISPR/Cas9 technology in tilapia to further elucidate the relationship between GSK3β-controlled metabolic programs and T cell immunity.

Importantly, we proposed a novel notion that GSK3β had reshaped the strategy of regulating T cell immunity via metabolic programs, acquiring dual-efficacy pathways to determine T cell response, which enhances the flexibility of the adaptive immune system in mammals. Unlike the model that one site regulates one metabolism in bony fish, phosphorylation of Tyr216 site in mouse GSK3β enhanced two metabolic pathways simultaneously. This may suggest that, when energy demand increases, such as during T cell activation, this model responds more quickly by simultaneously boosting glycolysis and OXPHOS, thereby meeting the demand for intermediate metabolites and ATP. As energy demand further augments, mammalian GSK3β is able to initiate phosphorylation at both Tyr216 and Ser9, synergistically enhancing OXPHOS. When energy demand decreases, dephosphorylation of the Ser9 site reduces the intensity of OXPHOS. This model can be viewed as two switches: a large switch that rapidly activates both metabolisms and a smaller switch for following fine-tuning, ensuring high efficiency while minimizing energy waste. These findings may be associated to the mechanism redundancy between metabolic pathways, which prevent a single pathway malfunction

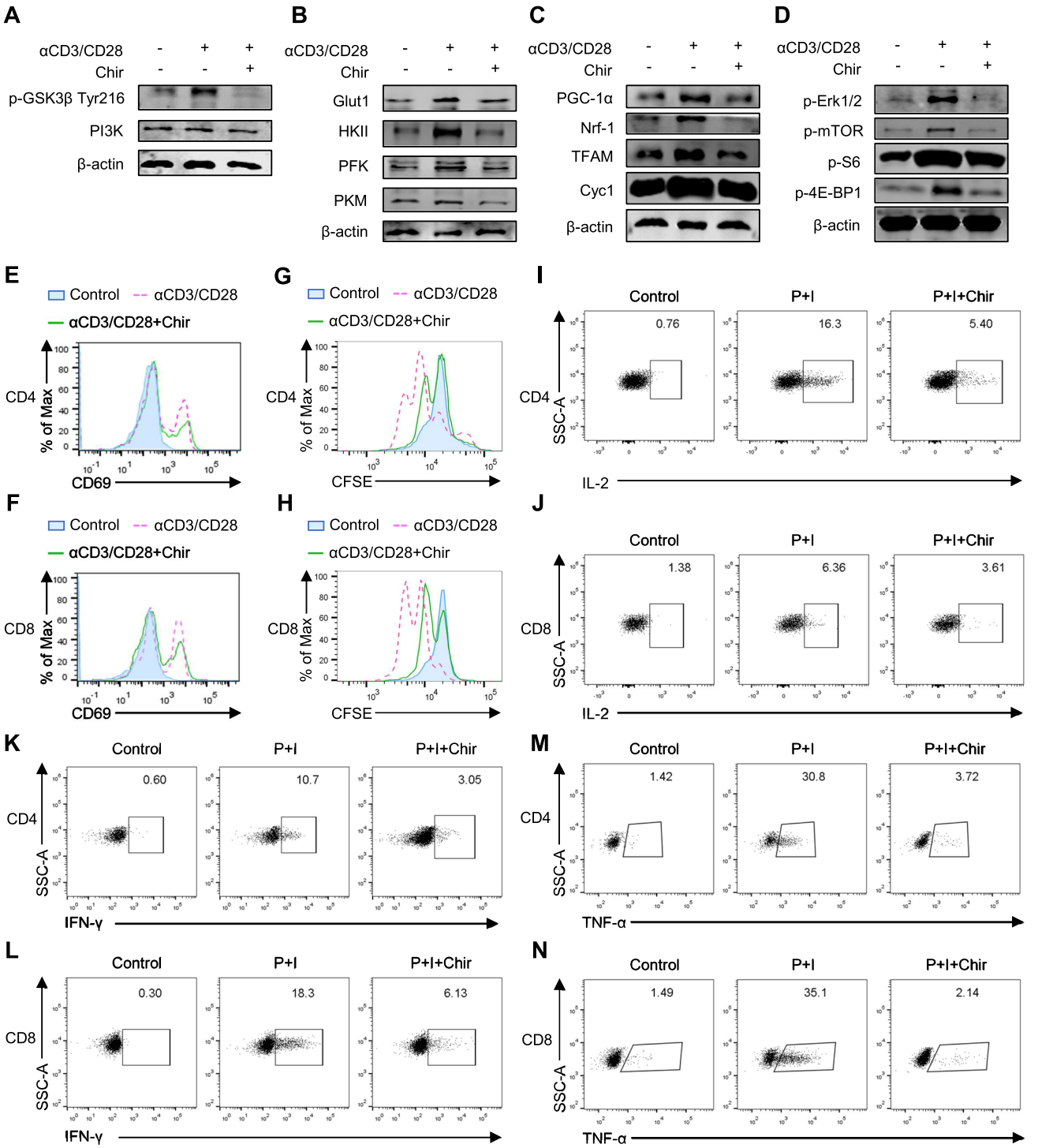

Fig. 6 GSK3β Tyr216 phosphorylation triggers glycolysis and OXPHOS to promote T cell response in mouse. **A**-**H** Mouse splenocytes were stimulated with CD3/CD28 mAbs in the presence or absence of the inhibitor Chir99021 for indicated time points. **A**-**D** Western blot showing the expression levels of indicated molecules at 6 h. **E**, **F** Histograms showing the CD69 expression levels in gated $CD4^+$ (**E**) or $CD8^+$ (**F**) T cells at 12 h. **G**, **H** Mouse splenocytes were labelled with CFSE and stimulated with CD3/CD28 mAbs. Histogram showing the proliferation of $CD4^+$ (**G**) or $CD8^+$ (**H**) T cells at 48 h. **I**-**N** Mouse splenocytes were stimulated with P+ I in the presence or absence of the inhibitor Chir99021 for 5 h. FACS plots showing the percentage of $CD4^+$ or $CD8^+$ T cells producing IL-2 (**I**, **J**), IFN-γ (**K**, **L**), or TNF-α (**M**, **N**). All the experiments were repeated for three independent times

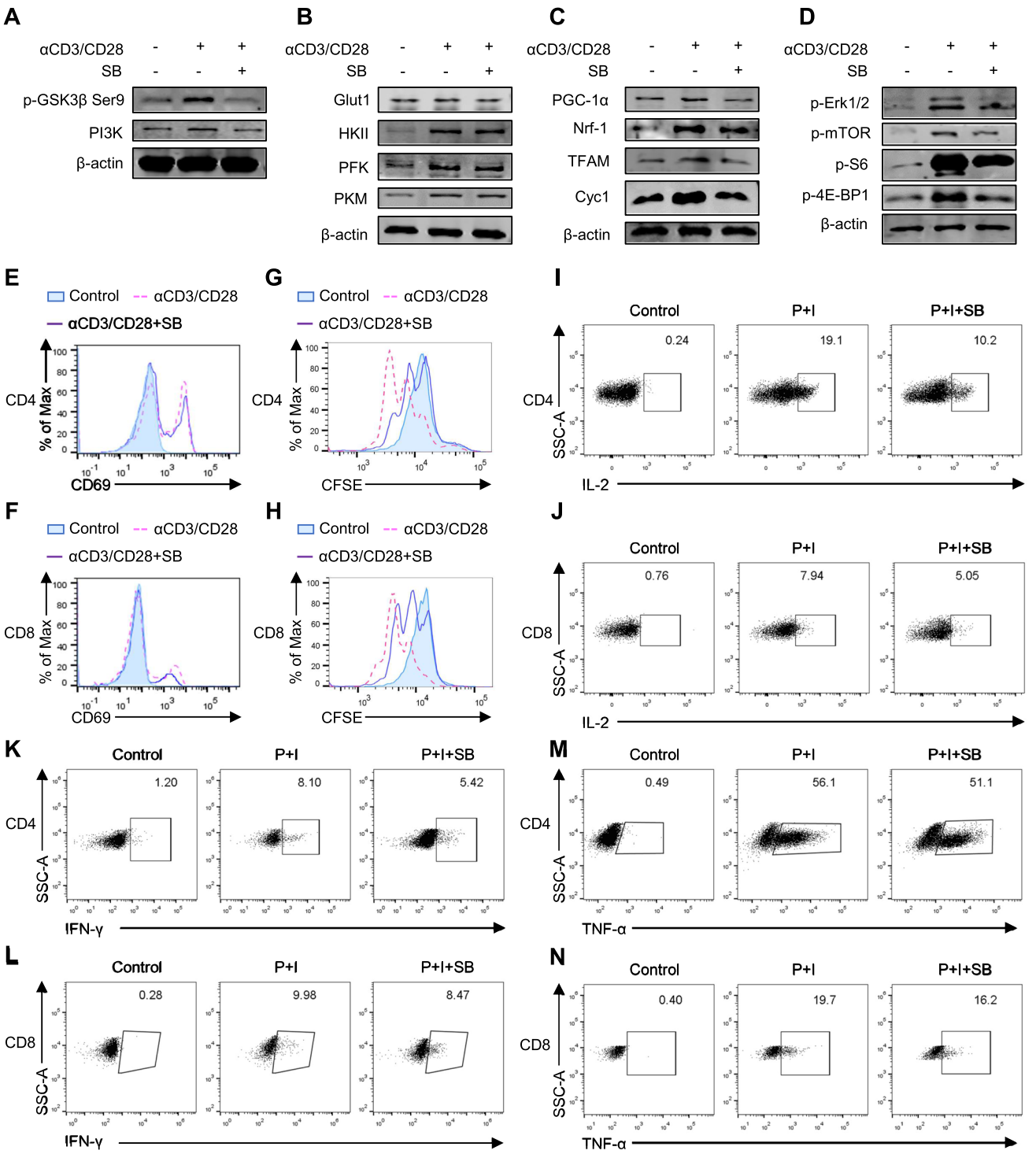

Fig. 7 Inhibition of Ser9 phosphorylation restrains T cell response via suppressing OXPHOS in mouse. **A-H** Mouse splenocytes were stimulated with CD3/CD28 mAbs in the presence or absence of the inhibitor SB216763 for indicated time points. **A-D** Western blot showing the expression levels of indicated molecules at 6 h. **E**, **F** Histograms showing the CD69 expression levels in gated $CD4^+$ (**E**) or $CD8^+$ (**F**) T cells at 12 h. **G**, **H** Mouse splenocytes were labelled with CFSE and stimulated with CD3/CD28 mAbs. Histogram showing the proliferation of $CD4^+$ (**G**) or $CD8^+$ (**H**) T cells at 48 h. **I-N** Mouse splenocytes were stimulated with P+ I in the presence or absence of the inhibitor SB216763 for 5 h. FACS plots showing the percentage of $CD4^+$ or $CD8^+$ T cells producing IL-2 (**I**, **J**), IFN-γ (**K**, **L**), or TNF-α (**M**, **N**). All the experiments were repeated for three independent times

from leading to immune system failure. This redundancy is important in evolution because pathogens may attempt to interfere with host metabolism, and the presence of multiple pathways increases resistance to interference, enhancing chances of survival. Therefore, the dual-site phosphorylation strategy of GSK3β likely endows higher vertebrates with more flexible metabolic regulation, allowing for rapid rewiring of metabolism to optimize T cell immunity in response to cellular states. This flexibility enables adaptation to changing environments and physiological demands. The strategy in Nile tilapia may be more effective under specific conditions, such as short-term, high-intensity energy demands, but it may lack the flexibility required for long-term adaptation and energy maintenance. This shift may represent the essence of adaptive immune reprogramming.

We attempted to understand the biological implications underlying GSK3β's remodeling of regulation in T cells from an evolutionary perspective. GSK3 regulates adaptive immunity in mammals [50], but it remains unknown whether this strategy is independently acquired by mammals or represents a common function gradually evolved in vertebrates. The fact that GSK3β coupled metabolic program to regulate T cell response in Nile tilapia, suggests this is a common strategy emerged prior to the tetrapod. Over hundreds of millions of years, vertebrates have evolved more complex immune mechanisms, and the regulatory role of GSK3β might have become increasingly pivotal. During this process, drastic changes in diet likely played a crucial role in altering the regulatory strategies of GSK3β in T cell immunity. It was indicated that the transition between functional and"exhausted"states of T cells was largely associated with changes in metabolic pathways of nutrition, particularly the shift from acetate metabolism to citrate metabolism [51]. This shift profoundly affected the identity and function of T cells, reflecting the complex relationship between the immune system and nutritional status. In Nile tilapia, a carbohydrate-rich diet promoted the phosphorylation of Ser12 on PPARα, whereas fasting inhibited this phosphorylation [52, 53], with GSK3β playing a critical upstream regulatory role [54]. It can be inferred that long-term dietary changes likely drive the reshaping of the GSK3β-mediated network in T cell immunity, thereby influencing the pattern of immune response. However, further studies are still needed to address the reasons accounting for this remodeling.

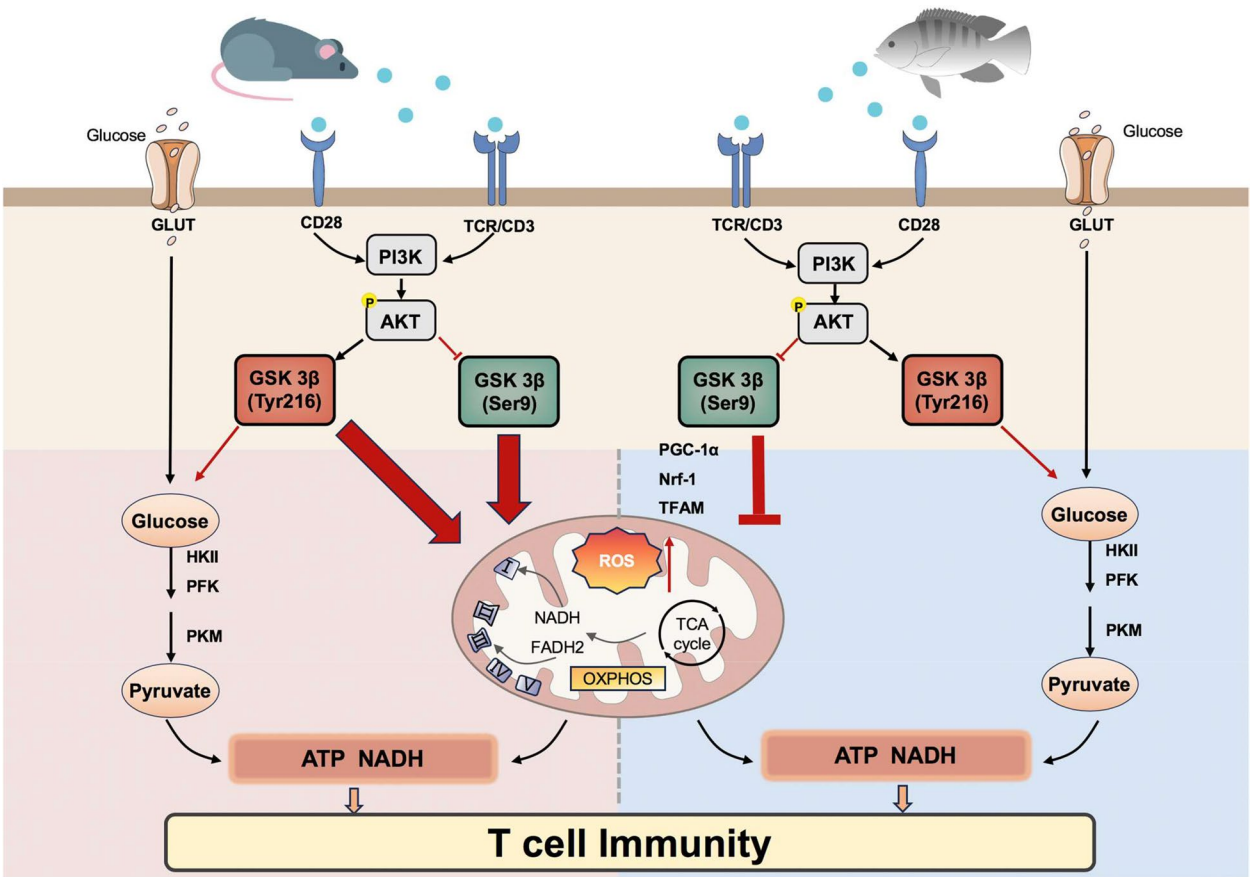

Fig. 8 Dual phosphorylation of GSK3β differentially coordinates metabolic programs to determine T cell immunity across vertebrates

In conclusion, we elucidated the mechanism that GSK3β specifically coordinates metabolism through dual-site phosphorylation to regulate T cell immunity in fish (Fig. 8). Intriguingly, in mice, this regulatory strategy of GSK3β had evolved, showing a distinct approach with enhanced efficiency and flexibility (Fig. 8). Therefore, we propose that during the evolutionary transition from lower to higher vertebrates, GSK3β reshaped its strategy for regulating T cell immunity through metabolic pathways, ultimately giving rise to a more sophisticated adaptive immune system. This sheds light on the mechanisms of T cell immunometabolism and the evolution of adaptive immune system.

Supplementary Information The online version contains supplementary material available at https://doi.org/10.1007/s00018-025-05746-1.

Acknowledgements We thank the Instrument-sharing Platform of the School of Life Sciences of East China Normal University (ECNU) for instrument sharing, the Flow Cytometry Core Facility of the School of Life Sciences of ECNU for the FACS analysis.

Author contribution W.L. performed experiments and drafted the manuscript. M.G. and W.R. drafted the manuscript. K.L. performed experiments and obtained the funding. YT.Z. drew the graph. YY.Z. helped to manage the project. X.W. and J.Y. obtained the funding, conceived the project and drafted the manuscript.

Funding This study was supported by grants from National Natural Science Foundation of China (No. 32373165, No. 32403068), Natural Science Foundation of Shanghai (24ZR1419700) and Shanghai Sailing Program (24YF2710300).

Data availability All data needed to evaluate the conclusions in the paper are present in the paper or the Supplementary Materials.

Declarations

Ethics approval All animal experiments were conducted in accordance with the guidelines for the Care and Use of Laboratory Animals of the Ministry of Science and Technology of China, and approved by the East China Normal University Experimental Animal Ethics Committee with an approve number of f+ m 20240703. All efforts were made to minimize the pain of animals.

Consent to participate The study does not contain clinical studies or patient data.

Consent to publish Not applicable.

Competing interests The authors declare no competing interests.

References

1. Dong C (2021) Cytokine regulation and function in T cells. Annu Rev Immunol 39:51–76. https://doi.org/10.1146/annurev-immunol-061020-053702
2. Chapman NM, Boothby MR, Chi H (2020) Metabolic coordination of T cell quiescence and activation. Nat Rev Immunol 20(1):55–70. https://doi.org/10.1038/s41577-019-0203-y
3. Frauwirth KA, Thompson CB (2004) Regulation of T lymphocyte metabolism. J Immunol 172(8):4661–4665. https://doi.org/10.4049/jimmunol.172.8.4661
4. Buck MD, O'Sullivan D, Pearce EL (2015) T cell metabolism drives immunity. J Exp Med 212(9):1345–1360. https://doi.org/10.1084/jem.20151159
5. Marelli-Berg FM, Fu H, Mauro C (2012) Molecular mechanisms of metabolic reprogramming in proliferating cells: implications for T-cell-mediated immunity. Immunology 136(4):363–369. https://doi.org/10.1111/j.1365-2567.2012.03583.x
6. Caro-Maldonado A, Gerriets VA, Rathmell JC (2012) Matched and mismatched metabolic fuels in lymphocyte function. Semin Immunol 24(6):405–413. https://doi.org/10.1016/j.smim.2012.12.002
7. Klysz D, Tai X, Robert PA, Craveiro M, Cretenet G, Oburoglu L et al (2015) Glutamine-dependent α-ketoglutarate production regulates the balance between T helper 1 cell and regulatory T cell generation. Sci Signal 8(396):ra97. https://doi.org/10.1126/scisignal.aab2610
8. Michalek RD, Gerriets VA, Jacobs SR, Macintyre AN, MacIver NJ, Mason EF et al (2011) Cutting edge: distinct glycolytic and lipid oxidative metabolic programs are essential for effector and regulatory CD4+ T cell subsets. J Immunol 186(6):3299–3303. https://doi.org/10.4049/jimmunol.1003613
9. Shi LZ, Wang R, Huang G, Vogel P, Neale G, Green DR et al (2011) HIF1alpha-dependent glycolytic pathway orchestrates a metabolic checkpoint for the differentiation of TH17 and Treg cells. J Exp Med 208(7):1367–1376. https://doi.org/10.1084/jem.20110278
10. Palmer CS, Ostrowski M, Balderson B, Christian N, Crowe SM (2015) Glucose metabolism regulates T cell activation, differentiation, and functions. Front Immunol 6:1. https://doi.org/10.3389/fimmu.2015.00001
11. Doble BW, Woodgett JR (2003) GSK-3: tricks of the trade for a multi-tasking kinase. J Cell Sci 116(Pt 7):1175–1186. https://doi.org/10.1242/jcs.00384
12. Beurel E, Grieco SF, Jope RS (2015) Glycogen synthase kinase-3 (GSK3): regulation, actions, and diseases. Pharmacol Ther 148:114–131. https://doi.org/10.1016/j.pharmthera.2014.11.016
13. Buller CL, Loberg RD, Fan MH, Zhu Q, Park JL, Vesely E et al (2008) A GSK-3/TSC2/mTOR pathway regulates glucose uptake and GLUT1 glucose transporter expression. Am J Physiol Cell Physiol 295(3):C836-843. https://doi.org/10.1152/ajpcell.00554.2007
14. Yang K, Chen Z, Gao J, Shi W, Li L, Jiang S et al (2017) The Key Roles of GSK-3β in Regulating Mitochondrial Activity. Cell Physiol Biochem 44(4):1445–1459. https://doi.org/10.1159/000485580

15. Fang G, Zhang P, Liu J, Zhang X, Zhu X, Li R et al (2019) Inhibition of GSK-3β activity suppresses HCC malignant phenotype by inhibiting glycolysis via activating AMPK/mTOR signaling. Cancer Lett 463:11–26. https://doi.org/10.1016/j.canlet.2019.08.003
16. Tsai CC, Tsai CK, Tseng PC, Lin CF, Chen CL (2020) Glycogen synthase kinase-3β facilitates cytokine production in 12-O-tetradecanoylphorbol-13-acetate/ionomycin-activated human CD4(+) T lymphocytes. Cells 9(6). https://doi.org/10.3390/cells9061424
17. Garcia CA, Benakanakere MR, Alard P, Kosiewicz MM, Kinane DF, Martin M (2008) Antigenic experience dictates functional role of glycogen synthase kinase-3 in human CD4+ T cell responses. J Immunol 181(12):8363–8371. https://doi.org/10.4049/jimmunol.181.12.8363
18. Taylor A, Harker JA, Chanthong K, Stevenson PG, Zuniga EI, Rudd CE (2016) Glycogen synthase kinase 3 inactivation drives T-bet-mediated downregulation of Co-receptor PD-1 to enhance CD8(+) cytolytic T cell responses. Immunity 44(2):274–286. https://doi.org/10.1016/j.immuni.2016.01.018
19. Miyazawa R, Murata N, Matsuura Y, Shibasaki Y, Yabu T, Nakanishi T (2018) Peculiar expression of CD3-epsilon in kidney of ginbuna crucian carp. Front Immunol 9:1321. https://doi.org/10.3389/fimmu.2018.01321
20. Ai K, Li K, Jiao X, Zhang Y, Li J, Zhang Q et al (2022) IL-2-mTORC1 signaling coordinates the STAT1/T-bet axis to ensure Th1 cell differentiation and anti-bacterial immune response in fish. PLoS Pathog 18(10):e1010913. https://doi.org/10.1371/journal.ppat.1010913
21. Zhang J, Wang X, Li K, Rao W, Jiao X, Liang W et al (2024) Hyperosmotic stress induces inflammation and excessive Th17 response to blunt T-cell immunity in Tilapia. J Immunol 212(12):1877–1890. https://doi.org/10.4049/jimmunol.2300251
22. Hui SP, Sugimoto K, Sheng DZ, Kikuchi K (2022) Regulatory T cells regulate blastemal proliferation during zebrafish caudal fin regeneration. Front Immunol 13:981000. https://doi.org/10.3389/fimmu.2022.981000
23. Mu P, Huo J, Li X, Li W, Li X, Ao J et al (2022) IL-2 signaling couples the MAPK and mTORC1 axes to promote T cell proliferation and differentiation in Teleosts. J Immunol 208(7):1616–1631. https://doi.org/10.4049/jimmunol.2100764
24. Wei X, Li H, Zhang Y, Li C, Li K, Ai K et al (2020) Ca(2+)-calcineurin axis-controlled NFAT nuclear translocation is crucial for optimal T cell immunity in an early vertebrate. J Immunol 204(3):569–585. https://doi.org/10.4049/jimmunol.1901065
25. Wei X, Li C, Zhang Y, Li K, Li J, Ai K et al (2021) Fish NF-κB couples TCR and IL-17 signals to regulate ancestral T-cell immune response against bacterial infection. Faseb J 35(4):e21457. https://doi.org/10.1096/fj.202002393RR
26. Wei X, Ai K, Li H, Zhang Y, Li K, Yang J (2019) Ancestral T cells in fish require mTORC1-coupled immune signals and metabolic programming for proper activation and function. J Immunol 203(5):1172–1188. https://doi.org/10.4049/jimmunol.1900008
27. Wei X, Zhang Y, Li C, Ai K, Li K, Li H et al (2020) The evolutionarily conserved MAPK/Erk signaling promotes ancestral T-cell immunity in fish via c-Myc-mediated glycolysis. J Biol Chem 295(10):3000–3016. https://doi.org/10.1074/jbc.RA119.012231
28. Li K, Wei X, Jiao X, Deng W, Li J, Liang W et al (2023) Glutamine metabolism underlies the functional similarity of T cells between nile Tilapia and Tetrapod. Adv Sci (Weinh) 10(12):e2201164. https://doi.org/10.1002/advs.202201164
29. Gu Y, Gao L, Han Q, Li A, Yu H, Liu D et al (2019) GSK-3β at the crossroads in regulating protein synthesis and lipid deposition in Zebrafish. Cells 8(3). https://doi.org/10.3390/cells8030205
30. Wang Y, Zhan X, Luo W, Zhao L, Yang S, Chen D et al (2019) GSK3β inhibition suppresses the hepatic lipid accumulation in Schizothorax prenanti. Fish Physiol Biochem 45(6):1953–1961. https://doi.org/10.1007/s10695-019-00691-w
31. Liu D, Mai K, Zhang Y, Xu W, Ai Q (2016) GSK-3b participates in the regulation of hepatic lipid deposition in large yellow croaker (Larmichthys crocea). Fish Physiol Biochem 42(1):379–388. https://doi.org/10.1007/s10695-015-0145-7
32. Liu D, Yu H, Gu Y, Pang Q (2021) Effect of rare earth element lanthanum on lipid deposition and Wnt10b signaling in the liver of male zebrafish. Aquat Toxicol 240:105994. https://doi.org/10.1016/j.aquatox.2021.105994
33. Li K, Wei X, Li K, Zhang Q, Zhang J, Wang D et al (2023) Dietary restriction to optimize T cell immunity is an ancient survival strategy conserved in vertebrate evolution. Cell Mol Life Sci 80(8):219. https://doi.org/10.1007/s00018-023-04865-x
34. Liang W, Li K, Gao H, Li K, Zhang J, Zhang Q et al (2024) Full T-cell activation and function in teleosts require collaboration of first and co-stimulatory signals. Zool Res 45(1):13–24. https://doi.org/10.24272/j.issn.2095-8137.2023.053
35. Gerriets VA, Rathmell JC (2012) Metabolic pathways in T cell fate and function. Trends Immunol 33(4):168–173. https://doi.org/10.1016/j.it.2012.01.010
36 Kamalam BS, Medale F, Panserat S (2017) Utilisation of dietary carbohydrates in farmed fishes: New insights on influencing factors, biological limitations and future strategies. Aquaculture 467:3–27. https://doi.org/10.1016/j.aquaculture.2016.02.007
37. Undi RB, Gutti U, Gutti RK (2017) LiCl regulates mitochondrial biogenesis during megakaryocyte development. J Trace Elem Med Biol 39:193–201. https://doi.org/10.1016/j.jtemb.2016.10.003
38. Pansters NA, van der Velden JL, Kelders MC, Laeremans H, Schols AM, Langen RC (2011) Segregation of myoblast fusion and muscle-specific gene expression by distinct ligand-dependent inactivation of GSK-3β. Cell Mol Life Sci 68(3):523–535. https://doi.org/10.1007/s00018-010-0467-7
39. Sutherland C, Leighton IA, Cohen P (1993) Inactivation of glycogen synthase kinase-3 beta by phosphorylation: new kinase connections in insulin and growth-factor signalling. Biochem J 296 (Pt 1)(Pt 1):15–19. https://doi.org/10.1042/bj2960015
40. Theeuwes WF, Gosker HR, Langen RCJ, Verhees KJP, Pansters NAM, Schols A et al (1863) (2017) Inactivation of glycogen synthase kinase-3β (GSK-3β) enhances skeletal muscle oxidative metabolism. Biochim Biophys Acta Mol Basis Dis 12:3075–3086. https://doi.org/10.1016/j.bbadis.2017.09.018
41. Geltink RIK, Kyle RL, Pearce EL (2018) Unraveling the complex interplay between T cell metabolism and function. Annu Rev Immunol 36:461–488. https://doi.org/10.1146/annurev-immunol-042617-053019
42 Lin J, Song T, Li C, Mao W (2020) GSK-3β in DNA repair, apoptosis, and resistance of chemotherapy, radiotherapy of cancer. Biochimica Et Biophysica Acta. Mol Cell Res 1867(5):118659. https://doi.org/10.1016/j.bbamcr.2020.118659
43. Yun S-I, Yoon H-Y, Chung Y-S (2009) Glycogen synthase kinase-3beta regulates etoposide-induced apoptosis via Bcl-2 mediated caspase-3 activation in C3H10T1/2 cells. Apoptosis: An Int J Programmed Cell Death 14(6):771–777. https://doi.org/10.1007/s10495-009-0348-4
44. Medunjanin S, Schleithoff L, Fiegehenn C, Weinert S, Zuschratter W, Braun-Dullaeus RC (2016) GSK-3β controls NF-kappaB activity via IKKγ/NEMO. Sci Rep 6:38553. https://doi.org/10.1038/srep38553
45. Steinbrecher KA, Wilson W, Cogswell PC, Baldwin AS (2005) Glycogen synthase kinase 3beta functions to specify gene-specific, NF-kappaB-dependent transcription. Mol Cell Biol 25(19):8444–8455. https://doi.org/10.1128/MCB.25.19.8444-8455.2005

46. Liao J, Zhang X, Zhang L, Xu Z, Kang S, Xu L et al (2022) Characterization and functional analysis of GSK3β from Epinephelus coioides in Singapore grouper iridovirus infection. Fish Shellfish Immunol 131:549–558. https://doi.org/10.1016/j.fsi.2022.10.024
47. Xu Y-C, Pantopoulos K, Zheng H, Zito E, Zhao T, Tan X-Y et al (2023) Phosphorus overload promotes hepatic lipolysis by suppressing GSK3β-dependent phosphorylation of PPARα at Ser84 and Thr265 in a freshwater teleost. Environ Sci Technol 57(6):2351–2361. https://doi.org/10.1021/acs.est.2c06330
48. Chang C-H, Curtis JD, Maggi LB, Faubert B, Villarino AV, O'Sullivan D et al (2013) Posttranscriptional control of T cell effector function by aerobic glycolysis. Cell 153(6):1239–1251. https://doi.org/10.1016/j.cell.2013.05.016
49. Sena LA, Li S, Jairaman A, Prakriya M, Ezponda T, Hildeman DA et al (2013) Mitochondria are required for antigen-specific T cell activation through reactive oxygen species signaling. Immunity 38(2):225–236. https://doi.org/10.1016/j.immuni.2012.10.020
50. Beurel E, Michalek SM, Jope RS (2010) Innate and adaptive immune responses regulated by glycogen synthase kinase-3 (GSK3). Trends Immunol 31(1):24–31. https://doi.org/10.1016/j.it.2009.09.007
51. Ma S, Dahabieh MS, Mann TH, Zhao S, McDonald B, Song W-S et al (2025) Nutrient-driven histone code determines exhausted CD8+ T cell fates. Science (New York, N.Y.) 387(6734):eadj3020. https://doi.org/10.1126/science.adj3020
52. Luo Y, Hu C-T, Qiao F, Wang X-D, Qin JG, Du Z-Y et al (2020) Gemfibrozil improves lipid metabolism in Nile tilapia Oreochromis niloticus fed a high-carbohydrate diet through peroxisome proliferator activated receptor-α activation. Gen Comp Endocrinol 296:113537. https://doi.org/10.1016/j.ygcen.2020.113537
53. Ning L-J, He A-Y, Li J-M, Lu D-L, Jiao J-G, Li L-Y et al (1861) 2016) Mechanisms and metabolic regulation of PPARα activation in Nile tilapia (Oreochromis niloticus. Biochimica Et Biophysica Acta 1036:9 Pt A– 1048. https://doi.org/10.1016/j.bbalip.2016.06.005
54. Hinds TD, Burns KA, Hosick PA, McBeth L, Nestor-Kalinoski A, Drummond HA et al (2016) Biliverdin reductase a attenuates hepatic steatosis by inhibition of glycogen synthase kinase (GSK) 3β phosphorylation of serine 73 of peroxisome proliferator-activated receptor (PPAR) α. J Biol Chem 291(48):25179–25191. https://doi.org/10.1074/jbc.M116.731703